

ULTRASONIC ABSORPTION IN POLYMER SOLUTIONS

By

HIROYASU NOMURA, SHIGEO KATO and YUTAKA MIYAHARA

Department of Chemical Engineering

(Received June 14, 1975)

CONTENTS

	Page
1. Introduction	73
2. Theories	74
2.1. Propagation of Sound and Visco-elastic Constants	74
2.2. Thermodynamic Theory of Relaxation	75
2.3. Propagation of Sound and Relaxation Equations	76
2.4. Two-State Model	77
2.4.1. Thermal Relaxation in Ideal Mixtures	77
2.4.2. Volume Relaxation in Ideal Mixtures	78
2.4.3. Relaxation Frequency	78
3. Experimental	79
3.1. Ultrasonic Absorption Measurements	79
3.2. Determination of Relaxation Parameters	81
4. Experimental Results and Discussion	81
4.1. Ultrasonic Absorption and Relaxation Mechanism in Polyvinyl-type Polymer Solutions	81
4.1.1. Ultrasonic Relaxation in Solutions of Polystyrene	81
4.1.1.1. Effects of Molecular Weight on the Relaxation Mechanism	85
4.1.1.2. Effects of Solvents on the Relaxation Mechanism	90
4.1.1.3. Mechanism of Ultrasonic Relaxation in Polystyrene Solutions	91
4.1.2. Discussion on the Double Relaxation	96
4.1.3. Ultrasonic Relaxation in the KHz Range	98
4.1.4. Ultrasonic Relaxation of Polystyrene of Low Molecular Weight	98
4.2. Ultrasonic Relaxation in Solutions of Polyvinyl Acetate, Polyvinyl Propionate, and Polyvinyl Butylate	99
4.2.1. Effect of Side-chain-length on the Low Frequency side Relaxation Frequency	100
4.2.2. Mechanism of the High-frequency Side Relaxation	103
4.3. Ultrasonic Relaxation in Aqueous Solutions of Polyvinyl Pyrrolidone	104
4.4. Ultrasonic Relaxation in other Vinyl-Polymer Solutions	109
4.5. Ultrasonic Absorption in Solutions of Miscellaneous Polymers	111
4.5.1. Ultrasonic Absorption in Solutions of Polycarbonate	111
4.5.1.1. Dioxane Solutions	111
4.5.1.2. Chloroform Solutions	113

4.5.2. Aqueous Solutions of Polyethylene Glycol	115
4.5.3. Dextran and Cellulose Derivatives	116
4.6. Abnormal Behavior of Ultrasonic Relaxation caused by Changes in Conformation of Polymer Molecules	118
4.7. Compressional Modulus and Shear Modulus of Polymer Solutions	119
5. Conclusion	121

1. Introduction

The visco-elastic properties of dilute polymer solutions have been the subject of a number of papers appeared in the literature in these two decades. The frequencies used in the experiment of the dynamic visco-elastic properties have, however, been limited below 100 KHz. One of the reasons why not so much attention is paid in the high frequency range is, probably, the great success of the theory of Rouse-Zimm.

Recently, however, the existence of some viscositic force at high frequencies, other than the usual viscositic force between the beads of molecules of high molecular weight and the medium, has been suggested from the discrepancy between the theory of Rouse-Zimm and the results of more accurate experiments. The measurements of ultrasonic absorption in polymer solutions in megahertz region have shed some light on this and the other unsolved problems in the visco-elastic properties of polymer solutions in the high frequency range.

The earliest measurements of the ultrasonic absorption in polymer solutions were probably those made by Wada and Shimbo (56), who measured it in the solutions of polymethylmethacrylate in benzene. The similar experiments were reported by Gooberman (11) a little later. In these reports, the measurements were made at some fixed frequency, and no relaxation had yet been found. From 1961 to 1964, Cerf and his coworkers (5) made measurements on various polymer solutions in the frequency range from 1 to 10 MHz.

On the 6th International Congress of Acoustics held in Tokyo in 1968, two papers on the absorption of ultrasonic in polymer solutions measured in wide frequency range were read. One was by Hässler and Bauer and another by us, both of which confirmed the existence of relaxation mechanism in the megahertz range. These results were published as the full paper in 1969 on *Kolloid Z.* by Hässler and Bauer (14) and on *Nippon Kagaku Zasshi* by us (34). A series of systematic studies have been made in our laboratory thereafter.

The applications of ultrasonic absorption measurement on some topics are not few. For example, the helix-coil transition of polyamino acid solutions (4, 49) was studied by this method.

In the present paper, the results of the extensive study on the ultrasonic absorption in the polymer solutions made mainly in our laboratory are reviewed, and the mechanisms of relaxation process which gives rise to the ultrasonic absorption are discussed.

2. Theories

2. 1. Propagation of Sound and Visco-elastic Constants

In general, the amplitude of sound wave propagating in a material attenuates as the procession of the wave. The displacement of the material, u , caused by the sound is expressed as

$$u = u_0 e^{-\alpha x} e^{i\omega \left(t - \frac{x}{c}\right)} \quad (1)$$

$$\omega = 2\pi f \quad (2)$$

where α is the absorption coefficient. The absorption per wave length is defined as

$$\mu = \alpha \lambda \quad (3)$$

where λ is the wave length.

The propagation of sound with attenuating amplitude is expressed in terms of the complex velocity

$$u = u_0 e^{i(\omega t - k^* x)} = u_0 e^{i\omega \left(t - \frac{x}{c^*}\right)} \quad (4)$$

where C^* is the complex velocity, and k^* the propagation constant defined as

$$\frac{1}{C^*} = \frac{1}{C} - i \frac{\alpha}{\omega} \quad (5)$$

and

$$k^* = \frac{\omega}{C} - i\alpha \quad (6)$$

The complex longitudinal modulus, M^* , is defined as

$$Z^* = \rho C^* = (\rho M^*)^{1/2} \quad (7)$$

where ρ is the density, and Z^* the acoustic impedance.

For the sinusoidal time change, the storage modulus, M' , and the loss modulus, M'' , are given as

$$M'(\omega) \equiv \mathcal{R}(M^*) = M_0 + M_1 \frac{\omega^2 \tau_1^2}{1 + \omega^2 \tau_1^2} \quad (8)$$

and

$$M''(\omega) \equiv \mathcal{I}(M^*) = M_1 \frac{\omega \tau_1}{1 + \omega^2 \tau_1^2} \quad (9)$$

where M_0 is the equilibrium longitudinal modulus, and τ_1 the relaxation time.

For the isotropic media such as liquids and solutions, the complex longitudinal modulus M^* can be expressed in terms of the complex compressional modulus K^* and the complex shear modulus G^*

$$M^* = K^* + \frac{4}{3}G^* \quad (10)$$

The complex volume viscosity κ^* and the complex shear viscosity η^* are related to these moduli as

$$\kappa^* = \frac{K^*}{\omega} \quad (11)$$

and

$$\eta^* = \frac{G^*}{\omega} \quad (12)$$

The propagation velocity of sound and the absorption coefficient are related to these moduli in equations

$$M' = K' + \frac{4}{3}G' = \rho C_l^2 \frac{1 - (\alpha_l C_l / \omega)^2}{\{1 + (\alpha_l C_l / \omega)^2\}^2} \quad (13)$$

$$M'' = K'' + \frac{4}{3}G'' = \rho C_l^2 \frac{2(\alpha_l C_l / \omega)^2}{\{1 + (\alpha_l C_l / \omega)^2\}^2} \quad (14)$$

$$G' = \rho C_t^2 \frac{1 - (\alpha_t C_t / \omega)^2}{\{1 + (\alpha_t C_t / \omega)^2\}^2} \quad (15)$$

$$G'' = \rho C_t^2 \frac{2(\alpha_t C_t / \omega)^2}{\{1 + (\alpha_t C_t / \omega)^2\}^2} \quad (16)$$

where the suffix l refers to the longitudinal waves and t to the transverse waves.

2. 2. Thermodynamic Theory of Relaxation

The thermodynamic theory of absorption of sound has been well established by J. Lamb (22) on the basis of the thermodynamics of systems containing the internal ordering parameters. The complex adiabatic compressibility, β_s^* , is given as

$$\beta_s^*(i\omega) = \beta_s^0 \frac{1 + i\omega \frac{\beta_s^\infty}{\beta_s^0} \tau}{1 + i\omega \tau} \quad (17)$$

where τ is the relaxation time, and β_s^0 the equilibrium adiabatic compressibility. The relaxation strength r is defined as

$$r = \frac{\beta_s^0 - \beta_s^\infty}{\beta_s^0} = \frac{\partial \beta_s}{\beta_s^0} \quad (18)$$

where β_s^∞ is the instantaneous adiabatic compressibility.

2.3. Propagation of Sound and Relaxation Equations

The complex propagation constant, k^* , can be represented in terms of the complex compressibility in equations

$$\begin{aligned} \frac{k^{*2}}{\omega^2} &= \rho \beta_s^0 \left(1 + i \omega \frac{\beta_s^\infty}{\beta_s^0} \right) / (1 + i \omega \tau) \\ &= \rho \beta_s^0 \left\{ 1 - \frac{i \omega \tau}{1 + i \omega \tau} r \right\} \end{aligned} \quad (19)$$

From Eq. (19), we obtain the single relaxation equation

$$\frac{\alpha}{f^2} = \frac{A}{1 + \omega^2 \tau^2} = \frac{A}{1 + (f/f_r)^2} \quad (20)$$

$$A = \frac{2\pi^2}{C} \tau r \quad (21)$$

and

$$f_r = \frac{1}{2\pi\tau} \quad (22)$$

The absorption per wave length exhibits a maximum with respect to the frequency, which is given by

$$\omega_{\max} \tau = (1 - r)^{-1/2} \quad (23)$$

and its maximum value is

$$\mu_{\max} = 4\pi \left\{ \left[1 + \frac{1}{4} \frac{r^2}{(1-r)^2} \right]^{1/2} - 1 \right\} / \frac{r}{(1-r)^{1/2}} \quad (24)$$

The relation between r and μ_{\max} is

$$\frac{r}{(1-r)^{1/2}} = \frac{4(\mu_{\max}/2\pi)}{1 - (\mu_{\max}/2\pi)^2} \quad (25)$$

The relaxation strength can be given by the thermodynamic calculations as

$$\begin{aligned}
 r &= \frac{C_p^0}{C_p^\infty} \left[\left(\frac{\partial \beta_T}{\beta_s^0} \right)^{1/2} - \left\{ (\gamma - 1) \frac{\delta C_p}{C_p^0} \right\}^{1/2} \right]^2 \\
 &= \frac{(\gamma - 1)}{C_p^\infty} \delta C_p \left[1 - \frac{C_p^0 \Delta V}{V \theta \Delta H_0} \right]^2
 \end{aligned}
 \tag{26}$$

In Eq. (26), when $\delta \beta_T \simeq 0$ or $\Delta V \simeq 0$ and the first term in the bracket in the first equation is negligible, we call it the thermal relaxation, and when $\delta C_p \simeq 0$ or $\Delta H_0 \simeq 0$, and the second term in the bracket in the first equation is negligible, the volume relaxation.

2. 4. Two-State Model

The single-relaxation phenomena observed by the ultrasonic measurements in solutions are often ascribed to a two-state model. According to this model (Fig. 1.),

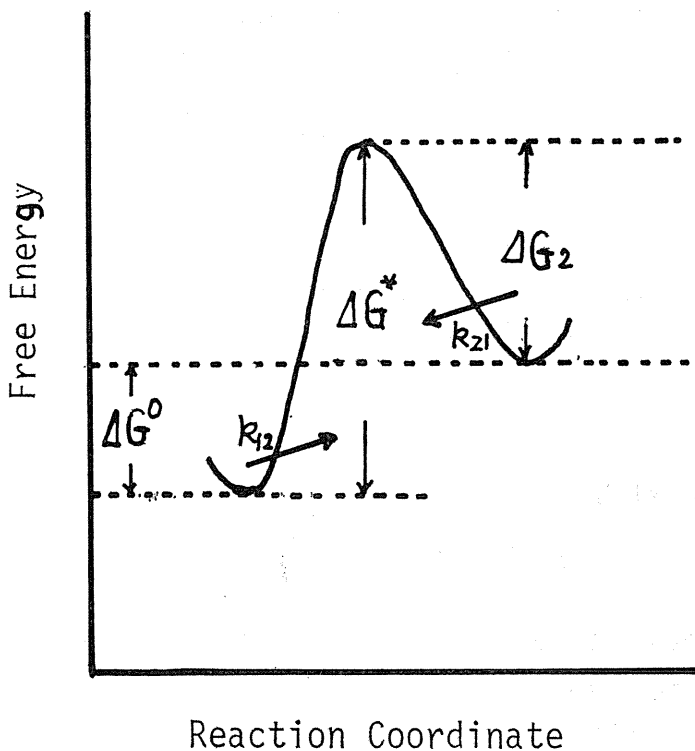


Fig. 1. Potential diagram for calculating the reaction rate ($A_1 \rightleftharpoons A_2$).

the ultrasonic absorption is originated from the disturbance of an equilibrium between two states by the external periodic perturbation.

2. 4. . Thermal Relaxation in Ideal Mixtures.

Consider a reaction



where k_{12} and k_{21} are the rate constants of the respective direction. Provided $r \ll 1$, the maximum of absorption per wave length, μ_{\max} , is given in terms of the standard enthalpy change, ΔH_0 , as

$$\frac{2\mu_{\max}}{\pi} \cdot \frac{C_p}{\gamma-1} = R \left(\frac{\Delta H_0}{RT} \right)^2 \frac{\exp(-\Delta G_0/RT)}{[1 + \exp(-\Delta G_0/RT)]^2} \quad (28)$$

Since ΔG_0 is related to ΔH_0 by the Gibbs-Helmholtz equation

$$\frac{\partial(\Delta G_0/T)}{\partial T} = -\frac{\Delta H_0}{T^2} \quad (29)$$

we can estimate ΔH_0 and ΔG_0 from the experimental values of μ_{\max} and C_p , at two different temperatures, and the standard entropy difference, ΔS_0 from the equation, $\Delta G_0 = \Delta H_0 - T \Delta S_0$. The γ can be obtained from the thermodynamic relation

$$(\gamma-1) = \frac{C^2 \theta^2 T}{C_p} \quad (30)$$

where C is the sound velocity and θ the expansibility.

2. 4. 2. Volume Relaxation in the Ideal Mixtures

When the volume relaxation is predominant, $\Delta H_0 = 0$, $\delta C_p = 0$, and from Eq. (26)

$$r = -\frac{C_p^0}{C_p^\infty} \frac{\delta \beta_T}{\beta_S} \quad (31)$$

Provided $r \ll 1$, and $C_p^0 \simeq C_p^\infty$, we have

$$r = \frac{\rho C^2}{RT} (\Delta V)^2 \frac{n_1^0 + n_2^0}{V} \frac{K}{(1+K)^2} \quad (32)$$

where K is the equilibrium constant, and $V/(n_1^0 + n_2^0)$ the apparent molar volume.

2. 4. 3. Relaxation Frequency

The relaxation time of the reaction (27) is given by

$$\tau = \frac{1}{k_{12} + k_{21}} \quad (33)$$

The transition probability between two states, A_1 and A_2 , can be written as

$$\Gamma_{21} = \frac{2\pi f_r}{1 + \exp(-\Delta G_0/RT)} \quad (34)$$

The activation enthalpy can be calculated from the equation

$$\Gamma_{21} = C \exp(-\Delta H_{21}/RT) \quad (35)$$

Actually, Γ_{21} at respective temperatures can be obtained from ΔG_0 which is estimated from the temperature change of μ_{\max} . The activation enthalpy can be calculated from the Arrhenius plot of $\ln \Gamma_{21}$ against $1/RT$ using Eq. (35).

3. Experimental

3.1. Ultrasonic Absorption Measurements.

The ultrasonic absorptions in solutions were measured by the pulse-echo technique. The accuracy of the absorption measurements was made sufficiently high to assure the significance in the excess absorption in dilute solutions. The measurable lowest concentration was about 1 g/100ml.

The solvents used varied in their ultrasonic absorption coefficient. The accuracy of the measurements was kept sufficiently high to assure the constant errors in the excess absorption coefficient $\Delta\alpha = \alpha - \alpha_0$ (α_0 is the absorption coefficient of pure solvent) for the solvents of high absorption coefficient such as benzene as well as for those of low absorption such as water.

The measuring frequency range was made as wide as possible, from 1 to 130 MHz. The covered frequency range was divided into three zones, 1 MHz-10MHz, 10MHz-20MHz, and 20MHz-130MHz.

Three types of apparatus were constructed for each frequency zone. The general fundamental block diagram is shown in Fig. 2. Details of the constructions

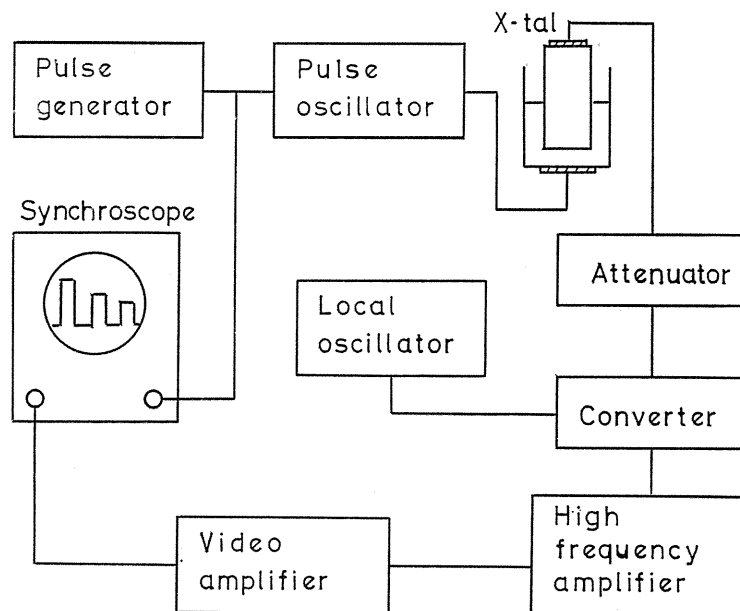


Fig. 2. Block diagram.

of apparatus are as follows.

- (1) 1 MHz-10MHz; A quartz crystal disk of fundamental resonance frequency of 1 MHz and 40 mm in diameter was used. The overtone frequencies of 3, 5, 7, 9 and 11 MHz were used for the measurements.
- (2) 10 MHz-20 MHz; The quartz crystal disks of fundamental resonance frequency of 2 and 3 MHz and 30 mm in diameter were used. The overtones of 6, 10, 14, 18, and 22 MHz of 2 MHz crystal and of 9, 15, and 21 MHz of 3 MHz crystal were used.

In these two apparatuses, the generation and receiving of ultrasonics were made by one crystal.

- (3) 20 MHz-130 MHz; The quartz crystal disks of fundamental resonance frequency of 4, 10 and 20 MHz were used. The diameter of disks was 20 mm. Their overtones were used for measurements. The signals were received by the separate crystal. A rod of fused quartz of 100 mm length and 20 mm in diameter was used as an ultrasonic delay line.

The measurements were made in the thermostats, the temperature of which was kept constant within the accuracy of $\pm 0.01^\circ\text{C}$. The measured temperatures are ranged from -50°C to 80°C .

As an illustrative example, the plots of readings of attenuator (dB) against the path length in toluene at 35°C and 20 MHz were shown in Fig. 3. From the slope of the straight line, the absorption coefficient can be estimated.

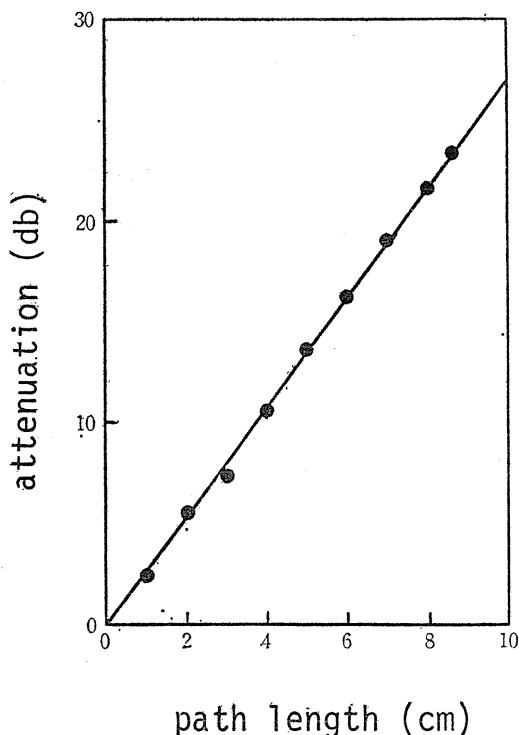


Fig. 3. Relationship between path length and attenuation.
(Toluene, 35°C)

For the measurements at the frequencies lower than 5 MHz, the correction for the diffraction was always made.

The measurements of ultrasonic velocities were made with the ultrasonic interferometers of 1 MHz and 4 MHz. The densities of solutions were measured with an Ostwald pycnometer of 20 ml in content.

3. 2. Determination of Relaxation Parameters.

The ultrasonic absorptions were measured at various frequencies and the various parameters in the relaxation equations were determined. For the curve-fitting, a computer, Hitach-10 was used. Before the measurements on solutions, the absence of relaxation was always confirmed by the ultrasonic absorption measurements on the pure solvent. Then, excess absorption parameters, $\Delta\alpha/f^2$, are plotted against $\log f$. The two constants, A and B , in the single relaxation equation

$$\frac{\Delta\alpha}{f^2} = \frac{A}{1 + (f/f_r)^2} + B \quad (36)$$

are determined by the curve-fitting using the computer. In the equation, the constant B includes such terms that come from the classical absorption. When the deviations from the curve amount to 5-8% over all frequency range, we give up the single-relaxation curve. We attempt to fit the observed results with double relaxation equation

$$\frac{\Delta\alpha}{f^2} = \frac{A_1}{1 + (f/f_{r1})^2} + \frac{A_2}{1 + (f/f_{r2})^2} + B \quad (37)$$

4. Experimental Results and Discussion

4. 1. Ultrasonic Absorption and Relaxation Mechanism in Polyvinyl-Type Polymer Solutions.

The concentration change of ultrasonic absorption was examined for solutions of various polyvinyl-type polymers. At the concentration lower than 15-20%, the plots of α/f^2 against the concentration, c , change linearly. As an illustrative example, the concentration dependence of α/f^2 for the solutions of polystyrene in M. E. K. (37) and polystyrene in D. B. Ph. (39) is shown in Figs. 4 and 5. As is shown in these figures, the linear relationship between α/f^2 and c is clear, and this relation hold true at all frequencies measured. Therefore, we can normalize the relative absorption parameter as $\alpha/f^2 c$.

4. 1. 1. Ultrasonic Relaxation in Solutions of Polystyrene

The ultrasonic absorption in the polystyrene solutions has been studied most thoroughly by us. In Table 1, the experimental results on the polystyrene solutions are summarized. In the table, the relaxation frequencies and μ_{\max} for various molecular weights in various solvents are shown. As is seen in the table, the double relaxation was reported in some solvents.

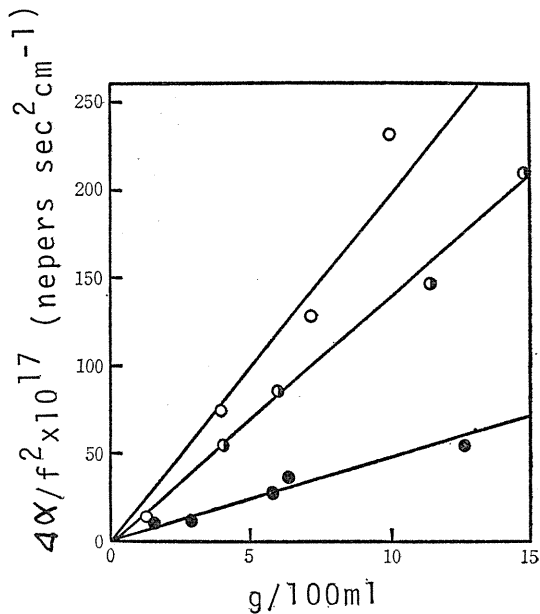


Fig. 4. Concentration dependence of ultrasonic absorption of polystyrene in M. E. K. at various frequencies. (20°C, ○ 8 MHz, ◐ 20 MHz, ● 47 MHz)

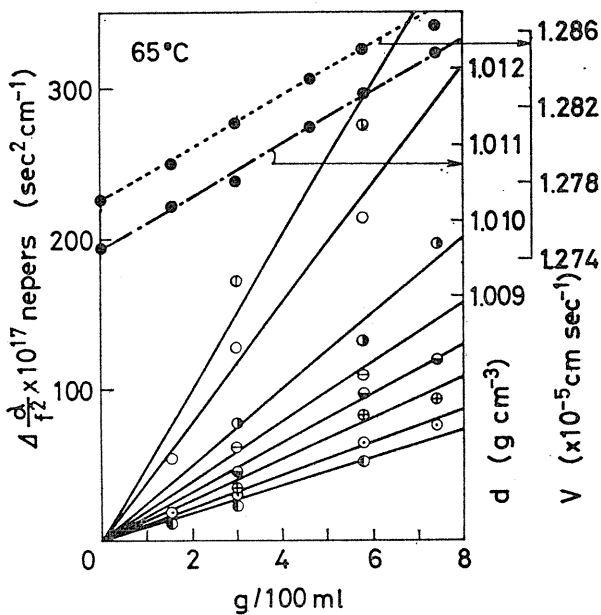


Fig. 5. Concentration dependence of ultrasonic absorption, velocity and density of solution at 25°C. (○ 3 MHz, ○ 6 MHz, ◐ 10 MHz, ◐ 12 MHz, ◐ 20 MHz, ◐ 28 MHz, ◐ 36 MHz, ◐ 52 MHz)

Table 1. Relaxation Parameters of Polystyrene in Various Solvents.

Solvent	M. W. $\times 10^4$	conc. g/dl	temp. °C	relaxation freq.		relaxation stren.		frequency ranges MHz	Ref.
				f_{r_1} MHz	f_{r_2} MHz	$\mu_{\max 1}$ $\times 10^{-3}$	$\mu_{\max 2}$ $\times 10^{-3}$		
Benzene	15.2	4	9	8.5		0.80		1—25	Hässler- Bauer.
			20	12.0		0.75			
	PS III	8	22	5.3		0.77			
		8	35	10.5		0.79			
	PS III C	10	20	10.5		1.54			
CCl ₄	43.0	5	10	3.0		1.08		1—25	Hässler- Bauer
			20	5.8		0.83			
	PS III C	5	35	9.2		0.61			
		5	20	6.6		0.85			
		10	3	2.3		1.97			
		10	20	6.2		1.77			
		10	40	11.5		1.57			
		10	60	17.7		1.45			
		20	20	6.0		3.70			
D. M. F	4.47	2.0	25	5.7	106.0	0.26	0.50	1—100	Ludlow et. al.
			25	5.4	77.0	0.34	0.69		
			25	5.0	71.0	0.56	1.20		
	9.82	2.5	25	7.3	76.0	0.39	0.69		
				6.9	75.0	0.38	0.69		
	17.3	2.0	25	5.9	86.0	0.24	0.48		
				5.4	73.0	0.29	0.61		
	30.0	2.5	25	5.6	79.0	0.36	0.68		
				5.3	74.0	0.40	0.95		
				7.2	87.0	0.55	0.94		
	4.5	25	25	6.9	94.0	0.63	1.10		
				5.4	69.0	0.57	1.13		
				4.8	82.0	0.22	0.52		
	41.1	2.0	25	7.6	78.0	0.40	0.68		
				5.4	90.0	0.23	0.50		
	86.7	2.0	25	5.0	75.0	0.36	0.77		
				5.0	75.0	0.36	0.77		
6.4				72.0	0.48	1.05			
25.0	3.0	25	5.8	35.0	0.32	0.40	1—150	Lemaréchal	
M. E. K	30	5.30	-20	8.2		1.019		1—60	Nomura et. al.
			-10	8.4		0.994			
			0	9.0		0.024			
			10	8.9		0.943			
			20	9.2		0.917			
			30	9.5		0.893			
	63.0	2.5	20	2.5	30.0	0.29	0.52	0.3—185	Ott. et. al.

Solvent	M. W. $\times 10^4$	conc. g/dl	temp. $^{\circ}\text{C}$	relaxation freq.		relaxation stre.		frequency ranges MHz	Ref.		
				f_{τ_1} MHz	f_{τ_2} MHz	$\mu_{\max 1}$ $\times 10^{-3}$	$\mu_{\max 2}$ $\times 10^{-3}$				
Decaline	30.0	3.02	10	9.6		0.742 ₁		1—60	Nomura et. al.		
			20	9.2		0.748 ₂					
			30	8.0		0.681 ₁					
			40	7.6		0.6508					
			50	6.5		0.5756					
			60	5.8		0.4816					
			70	5.3		0.4372					
			80	4.8		0.4036					
	63.0	2.5	20	1.3	30.0	0.60	0.78	0.3—185	Ott. et. al.		
	100.0	—	20	7.5	98.0	20.5*	34.6*	10—100	Ono. et. al.		
Xylene	100.0	—	20	3.4	46.0	8.5*	16.6*	0.1—100	Ono. et. al.		
D. E. Ph	63.0	2.5	20	0.80	10.0	0.43	0.75	0.3—185	Ott. et. al.		
D. B. Ph	30.0	5.79 ₁	15	1.5		0.899		1—60	Nomura et. al.		
			25	2.5		1.100					
			35	4.5		1.778					
			45	5.6		1.816					
			55	7.8		1.762					
			65	9.2		1.472					
	63.0	2.5	20	0.77	29.0	0.77	1.22	0.3—185	Ott. et. al.		
Toluene	0.21	2.70	0	23.0		0.518 ₄		3—130	Nomura et. al.		
			10	23.0		0.507 ₆					
			20	23.3		0.496 ₈					
			30	23.5		0.507 ₆					
			40	23.7		0.502 ₂					
			50	26.9		0.5400					
			0.40	2.61	0	19.6				0.459 ₄	
			10		20.0		0.430 ₇				
			20		20.3		0.433 ₃				
	30	18.7			0.412 ₄						
	40	19.9			0.409 ₈						
	50	19.0			0.407 ₂						
	30.0	4	-10	5.6		0.696					
			0	6.5		0.620					
			10	6.2		0.520					
			20	8.2		0.502					
			30	10.6		0.468					
			40	11.4		0.420					
			50	14.0		0.424					
30.0			6	-10	6.0		1.173		3—60	Nomura et. al.	
				0	7.4		1.034				

Solvent	M. W. $\times 10^4$	conc. g/dl	temp. $^{\circ}\text{C}$	relaxation freq.		relaxation stre.		frequency ranges MHz	Ref.
				f_{τ_1} MHz	f_{τ_2} MHz	$\mu_{\max 1}$ $\times 10^{-3}$	$\mu_{\max 2}$ $\times 10^{-3}$		
			10	9.0		0.888			
			20	10.4		0.779			
			30	12.0		0.735			
			40	18.0		0.738			
			50	18.0		0.710			
		8	-10	3.9		1.812			
			0	6.1		1.521			
			10	7.4		1.370			
			20	8.4		1.281			
			30	9.0		1.174			
			40	10.0		1.072			
			50	12.7		0.966			

4. 1. 1. 1. Effects of Molecular Weight on the Relaxation Mechanism.

The first report on the effect of molecular weight on the relaxation mechanism was given by Nomura and Miyahara in 1967 (33), and later on this problem was more exhaustively discussed by Nomura, Kato and Miyahara in 1973 (42). The experimental results on the solutions of polystyrene in toluene are shown in Fig. 6, where the molecular weights of polystyrene examined were 2,100, 4,000, 300,000, and 2,000,000. The temperature dependence of the relaxation curves for the polymer of molecular weight 4,000 and 300,000 is shown in Figs. 7 and 8.

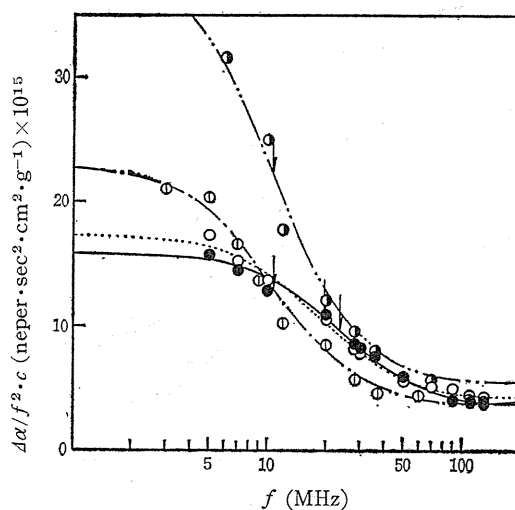


Fig. 6. Frequency dependence of ultrasonic absorption of polystyrene in toluene with various molecular weights.

(●) 2,100, ○ 4,000, ⊙ 300,000, ⊙ 2,000,000

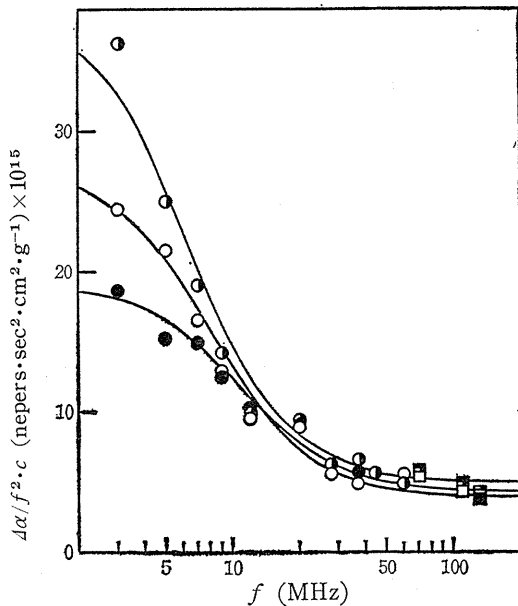


Fig. 7. Frequency dependence of ultrasonic absorption of polystyrene in toluene at various temperatures.
Molecular Weight; 300,000
Temperature ($^{\circ}\text{C}$) \bullet ; 40 \circ ; 20 \circ ; 0

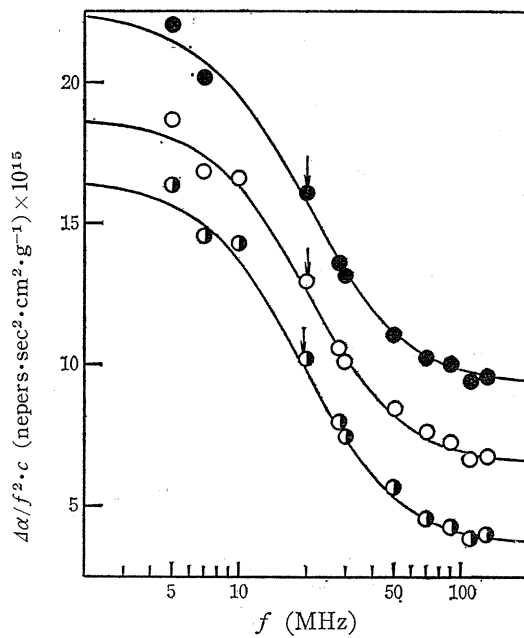


Fig. 8. Frequency dependence of ultrasonic absorption of polystyrene in toluene at various temperatures.
Molecular Weight; 4,000
Temperature ($^{\circ}\text{C}$) \bullet ; 40 \circ ; 20 \circ ; 0

As has already been shown in Figs. 6, 7 and 8, the single relaxation equation

$$\frac{\Delta\alpha}{f^2} = \frac{A}{1 + (f/f_r)^2} + B \quad (38)$$

is obeyed in the frequency range from 3 to 130 MHz at all temperatures measured.

The molecular weight dependence of the parameters, f_r , the relaxation frequency, A and B is shown in Figs. 9 and 10, and the temperature change of

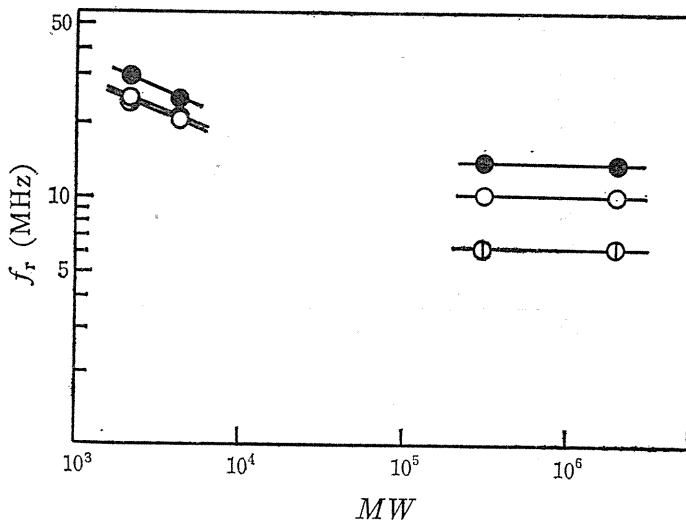


Fig. 9. Molecular weight dependence of relaxation frequencies at various temperatures.
Temperature ($^{\circ}\text{C}$) ●; 50, ○; 30, ⊖; 10

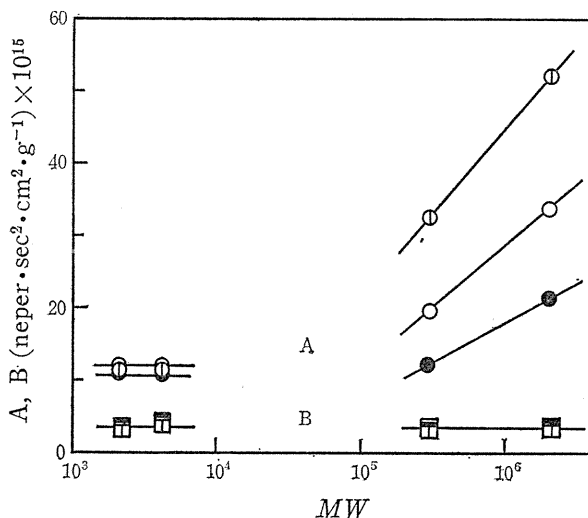


Fig. 10. Molecular weight dependence of single relaxation parameters of A and B at various temperatures.
Temperature ($^{\circ}\text{C}$) ● ■; 50, ○ □; 30, ⊖ □; 10

relaxation frequency is shown in Fig. 11.

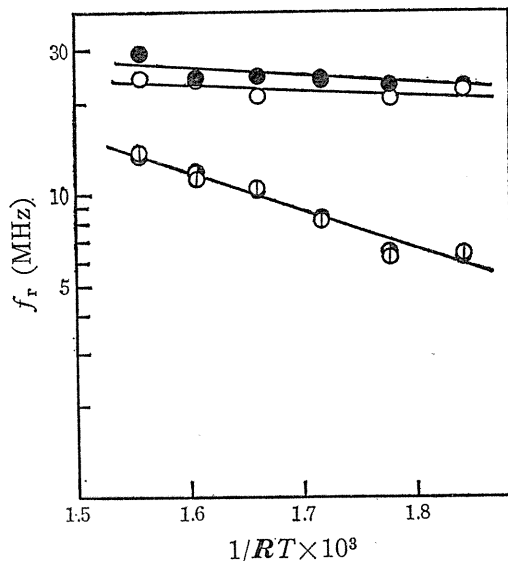


Fig. 11. Temperature dependence of relaxation frequencies of the polymers with various molecular weights.
Molecular Weight ●; 2,100, ○; 4,000, ⊙; 300,000
⊖; 2,000,000

The effect of molecular weight on the relaxation is summarized as follows.

- (1) The relaxation mechanism of polystyrene of high molecular weight is entirely different from that of low molecular weight.
- (2) For the polymer of molecular weight higher than 10,000, the relaxation frequency is independent of the molecular weight.

The apparent activation enthalpy, ΔH_{app} , obtained from the Arrhenius plot of f_r is also independent of molecular weight.

- (3) The constants A and B in the relaxation equation decrease with the increase in the molecular weight. The frequency dependence of the absorption per wave length, μ , is shown in Fig. 12, where $\Delta\mu/m$ is plotted against the frequency. As is seen in the figure, the relaxation strengths are

$$\mu_{\max} = 0.41 \times 10^3 \text{ mol}^{-1} \quad \text{for} \quad M = 20 \times 10^4$$

and

$$\mu_{\max} = 4.6 \times 10^4 \text{ mol}^{-1} \quad \text{for} \quad M = 200 \times 10^4.$$

Thus it is clear that the relaxation strength is proportional to the molecular weight.

The ultrasonic absorptions of solutions of polystyrene in xylene in the frequency range from 10 KHz were measured by Ohsawa and Wada (44) and Ono, Shintani, Yano and Wada (45) by the reverberation method. The results obtained by them are shown in Table 2 and Fig. 13. As is alleged by Ono, Shintani, Yano and Wada, the relaxation mechanism in this frequency range is entirely different from that in the megahertz range. The dependence of α/f^2 on the frequency is not represented

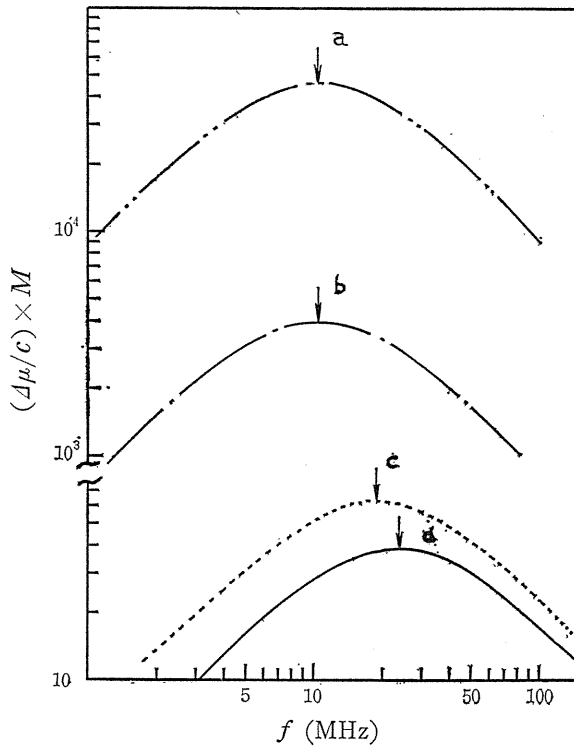


Fig. 12. Frequency dependence of absorption per wave length of the polymers with various molecular weights. Temperature; 30°C
Molecular Weight a; 2,000,000, b; 300,000, c; 4,000, d; 2,100

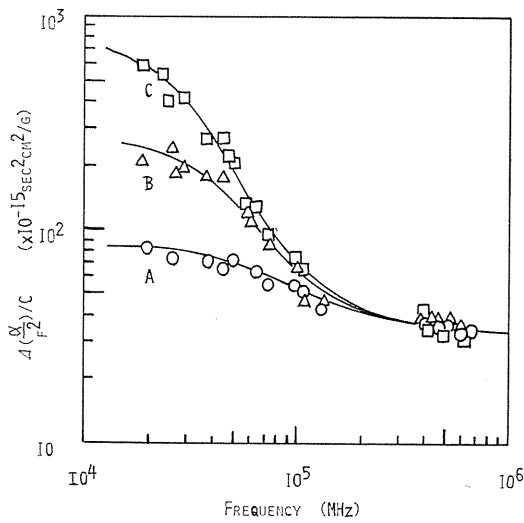


Fig. 13. Frequency dependence of ultrasonic absorption of three polystyrenes in xylene at 20°C.
Molecular Weight A; 2.1×10^5 , B; 3.7×10^5 , C; 10.0×10^5
(K. Ono et al. (45))

Table 2. Characteristic values for Low-frequency Relaxation of Polystyrene Solutions in xylene at 20°C (K. Ono, et al. (45))

Molecular weight 10^5	$[\eta]$ $10^2 \text{cm}^3/\text{g}$	$\Delta\alpha^2/f^2c$ $10^{-15} \text{sec}^2 \text{cm}^2/\text{g}$	f_r KHz
2.1	0.81	48	85
3.7	1.14	211	55
10.0	2.06	816	26

by the single relaxation equation. It shows a distribution of relaxation times, and the relaxation frequency depends on the molecular weight.

4. 1. 1. 2. Effects of Solvents on the Relaxation Mechanism.

In Table 1, it is noted that the solutions of polystyrene in D. M. F. show the double relaxation. The experimental results on the polystyrene-D. M. F. system obtained by Ludlow, Wyn-Jones and Rassing (26) and Lemaréchal (23) are shown in Fig. 14. Ludlow, Wyn-Jones and Rassing estimated the relaxation frequency of high frequency side to be 72 MHz, while Lemaréchal 35 MHz. This disagreement is probably due to the uncertainty in estimating the limiting value of B , $\lim_{f \rightarrow \infty} (\Delta\alpha/f^2) = B$.

The existence of double relaxation in the polystyrene solutions is also reported by several authors. Ono, Shintani, Yano and Wada (45) reported it in the solutions of xylene and decaline, and Ott, Michels and Lemaréchal (46) in M. E. K., decaline, D. E. Ph., and D. B. Ph.. The relaxation frequencies in decaline solutions reported by Ono, Shintani, Yano and Wada were $f_{r1} = 7.5$ MHz, and $f_{r2} = 98$ MHz, while those by Ott, Michels and Lemaréchal $f_{r1} = 1.3$ MHz and $f_{r2} = 30$ MHz. The value of f_r reported by Ono, Shintani, Yano and Wada was nearly in the same order of magnitude as that reported by us, $f_r = 9.2$ MHz.

The relation between the relaxation process and viscosities of the solvents used is shown in Table 3.

According to the Debye's theory of the dielectric relaxation, the relaxation time is given by

$$\tau = \frac{1}{2\pi f_r} = \frac{4\pi a^3 \eta}{kT} \quad (40)$$

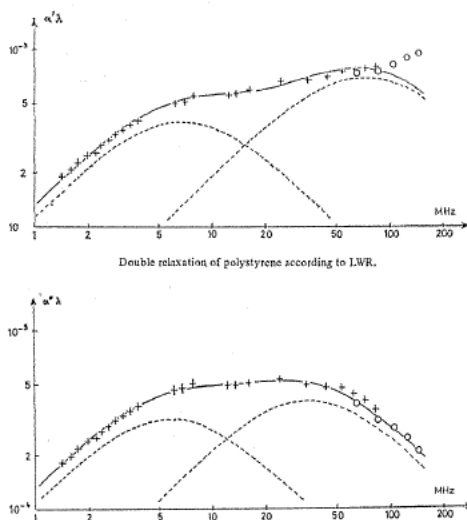


Fig. 14. Double relaxation of polystyrene in D. M. F. +; Ludlow et al. (26) o; Lemaréchal (23)

Table 3. Relaxation Frequencies and Viscosity of Solvents
(Molecular Weight 3.0×10^5 , 30°C)

Solvent	f_r MHz	η_0 c. p.	$\Delta H\eta$ Kcal/mol	ΔH_{21} Kcal/mol
toluene	10.6	0.522	0.41	2.57
M. E. K.	9.5	0.401	1.7	0.3
decaline	8.0	2.13	1.07	-2.57
D. B. Ph.	4.5	13.4	1.67	6.6
benzene*	10.0	0.56	0.88	6.6
CCl ₄ *	8.0	0.84	0.88	6.6

* Bauer et al (14)

where a is the diameter of molecules and η , the viscosity of solvent. If this equation could be applied to the ultrasonic relaxation of polystyrene solutions, the product of relaxation time and the viscosity would become constant, and the activation enthalpy of the relaxation time be same as that of the viscosity. In Table 3, the relaxation frequencies, the viscosities of solvents, and the activation enthalpy of relaxation are listed.

As is seen in the table, no consistent trend among these quantities is found to support the Debye's theory.

4. 1. 1. 3. Mechanism of Ultrasonic Relaxation in Polystyrene Solutions.

As is shown by a number of experimental evidences, the existence of a relaxation mechanism in the megahertz range in the polystyrene solutions seems to be undoubted. In the following, some characteristics of this relaxation are summarized.

- (1) This relaxation is single relaxation, or double at most. The plot of absorption parameter against the frequency can be represented satisfactorily by the equation of single or double relaxation. The relaxation curves form no such spectra with a distribution of relaxation times that are observed in a number of mechanical and electrical phenomena of polymer.
- (2) The relaxation frequencies in various solvents are independent of the molecular weight of the polystyrene.
- (3) The relaxation strength increases with the increase in the concentration as well as in the molecular weight. The magnitude of maximum absorption per wave length, μ_{\max} , is in the order 10^{-3} .

In general, the relaxation phenomena in liquids and solutions caused by the mechanical disturbance can be classified into following categories. (a) The structural relaxation. (b) The relaxation due to the viscosity. (c) The vibrational relaxation. (d) The rotational relaxation. (e) The relaxation caused by chemical reactions. Among them, the relaxation (e) can be excluded obviously as the origin of ultrasonic absorption in polystyrene solutions.

In Fig. 15, the spectra of μ of isobutyl bromide with respect to various types of relaxations are illustrated (25). As is seen in the figure, the relaxation frequencies of the structural, shear and vibrational relaxations lie in far higher frequency

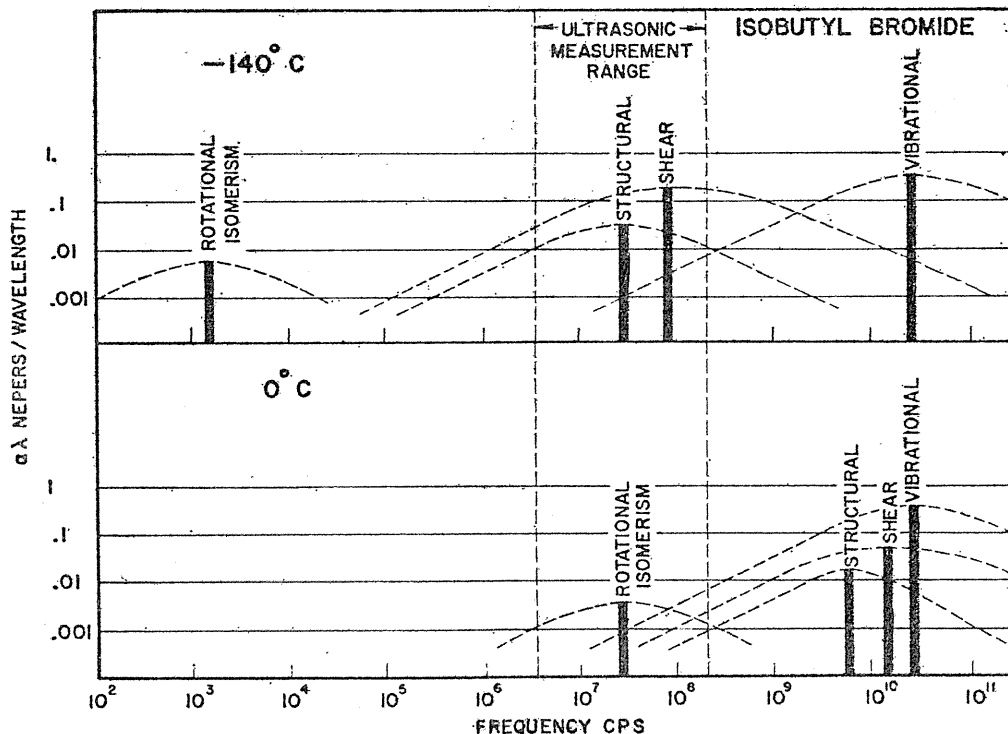


Fig. 15. Spectrograms of the loss per wave length in isobutyl bromide due to rotational isomerism, vibrational, shear and structural mechanisms. (T. A. Litovitz and C. M. Davis, (25))

range.

The mechanism (a) and (b) can be excluded as the origin of ultrasonic relaxation in polystyrene solutions for following reasons. (1) If this absorption is caused by the shear viscosity, the relaxation would not be single and the relaxation frequencies should exhibit a distribution as is predicted by the Rouse-Zimm theory of viscoelasticity. (2) The ultrasonic absorption caused by the viscosity is represented by the classical equation

$$\frac{\alpha}{f^2} = \frac{2\pi^2}{\rho C^3} \left(\kappa + \frac{4}{3}\eta \right) \quad (41)$$

where κ is the volume viscosity and η the shear viscosity. The experimental results showed that the value of α/f^2 is 10-100 times of that estimated from the κ and η (33). Furthermore, the relaxation strength estimated by this process would become 10-100 times higher than the experimental values. (cf. p. 119)

Judging from these facts, we assume that the ultrasonic relaxation in the polystyrene solutions is a thermal relaxation caused by the local rotational motions of groups of a few segments in the back-bone chain of polymer molecules in the solutions.

Hässler and Bauer (14) have suggested that the ultrasonic relaxation observed in the megahertz range is a thermal relaxation caused by the local rotation of a small part of molecular chains in the solutions. They assumed a motion of "Kink conformation" as the origin of thermal relaxation.

As a more natural model of local motion in the back-bone chain, we have proposed a model of crank-shaft motion as is shown in Fig. 16 (36). It is well known from the experimental results of X-ray diffraction that in crystal polystyrene molecules take the form of 3-fold screw. In the solutions, there are experimental supports that the molecules take partly the 3-fold screw structure (53, 3).

In our study, all of the samples of polystyrene used in the measurements shown in Table 1 are of atactic. It is, however, highly probable to assume that some local portion of the back-bone chains takes form of 3-fold screw in the solutions. The unit structure shown in Fig. 16 (a) is present in the back-bone chains in the solutions as their local structure, and an internal rotation on two C-C bonds, 1-2, and 7-8 is

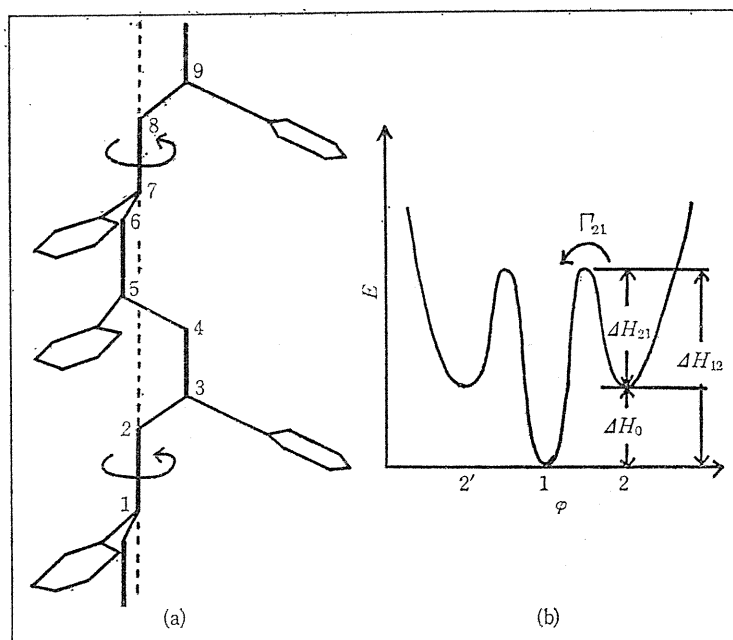


Fig. 16. Crank-Shaft model and variation of rotational energy.

possible. The change of potential energy with this internal rotations is shown in Fig. 16 (b). As is seen in Fig. 16(b), there are two states of different energies, which give rise to the thermal relaxation. This type of internal rotation does not change the valence angles, and the motion is limited in the motion of only four units. This motion gives no influence on the entire conformation of the molecule. The experimental data of ultrasonic relaxation of polystyrene solution can be explained satisfactorily on the basis of this crank-shaft motion. According to our crank-shaft motion model, the transition reaction to be considered is $(1) \rightleftharpoons (2)$, where the state (2) is doubly degenerated.

The decrement of heat capacity accompanied with the transition is

$$\delta C_p = R \left(\frac{\Delta H_0}{RT} \right)^2 \frac{2 \exp(-\Delta H_0/RT)}{\{1 + 2 \exp(-\Delta H_0/RT)\}^2} \quad (42)$$

where ΔH_0 is the enthalpy change of the transition. Provided $r \ll 1$, we have

$$\delta C_p \sim \frac{2\mu_{\max}}{\pi} \frac{C_p}{\gamma - 1} = \frac{2\mu_{\max}}{\pi} \frac{J}{T} \left(\frac{C_p}{C\theta} \right)^2 \quad (43)$$

The value of ΔH_0 can be estimated by the method of successive approximation. The values of δC_p at various temperatures are calculated from Eq. (42) at some assumed values of ΔH_0 . On the other hand, the temperature change of δC_p is also determined from Eq. (43) from the experimental measurements on the temperature change of μ_{\max} . By comparing these results, we can determine ΔH_0 .

As an illustrative example, the Arrhenius plot of δC_p for the solution of polystyrene in M. E. K. is shown in Fig. 17. Once the value of ΔH_0 is determined, the

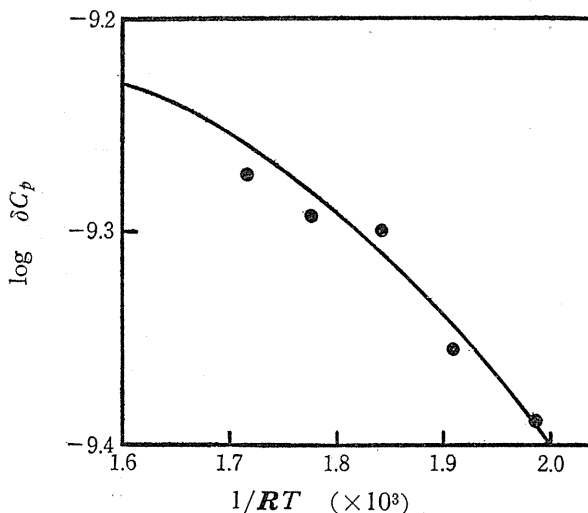


Fig. 17. Relation between δC_p and $1/RT$. (polystyrene-M. E. K.)

●; experimental.

—; calculated from Schottky equation.

transition probability between these two states, Γ_{21} , can be obtained from ΔH_0 and the relaxation frequency, f_r . The activation energy, ΔH_{21} , can be determined from the Arrhenius plot of Γ_{21} as is shown in Fig. 18 for the solution of polystyrene in M. E. K..

The potential height difference ΔH_0 and the activation enthalpy obtained are summarized in Table 4.

Bovey Hood, and Anderson (3) have reported that the $T-T$ type configuration of singiotactic molecule of polystyrene in the solutions is more stable than $T-G$

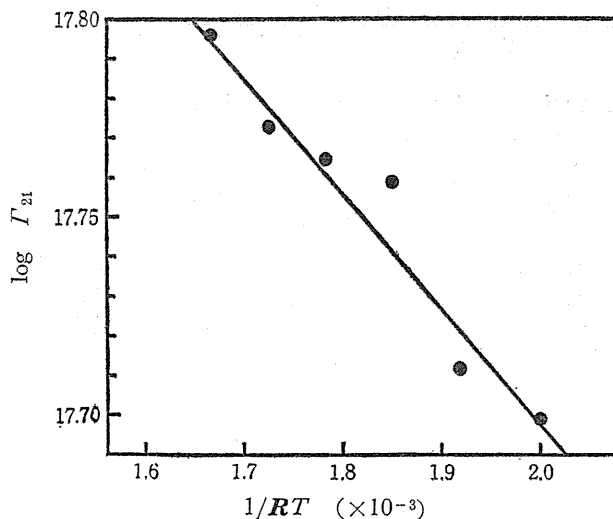


Fig. 18. Relation between transition rate and $1/RT$ (polystyrene-M. E. K.)

type, and the energy difference is about 1.7 kcal. This result does not contradict to ours.

The estimation of energy barrier and activation energy of this transition from the data of molecular force was tried. The $C-C$ axes, 1-2, and 7-8 in Fig. 16 (a) are fixed, and the phenyl radical is turned around on these axes. The values obtained were; $\Delta H_0 = 0.40$ kcal, and $\Delta H_{21} = 0.80$ kcal/mol. In the calculation, the interaction between following nine pairs are taken into account; Ph_1-Ph_3 , Ph_7-Ph_9 , Ph_5-Ph_3 , Ph_6-H_9 , $H_4^{(1)}-Ph_1$, $H_4^{(1)}-Ph_1$, H_7-Ph_9 , $H_8^{(8)}-Ph_9$, and $H_8^{(8)}-Ph_9$.

The intermolecular potentials are assumed to be the form

$$u(r) = 4 \epsilon \left\{ -\left(\frac{\sigma}{r}\right)^6 + \left(\frac{\sigma}{r}\right)^{12} \right\} \quad (44)$$

and the following values were assigned.

$C-C$ distance	1.42 Å
$C-H$ distance	1.08 Å
valence angle	108°43'

The values of constants in Eq. (44) used were;

	$\epsilon/k(\text{cal/mol})$	(Å)
$Ph-Ph$	440	200
$Ph-H$	129	200
$H-H$	38	200

Table 4. Activation Energies of Polystyrene in various Solvents.

Solvent	ΔH_0 Kcal/mol	ΔH_{21} Kcal/mol
Toluene	0.41	2.57
M. E. K.	1.7	0.3
Decaline	1.07	-2.57
D. B. Ph.	1.67	6.6
Benzene	0.88	6.6
CCl_4	0.88	6.6

The agreement between the calculated values and experimental results is excellent, and this result shows that our present model is highly plausible.

4. 1. 2. Discussion on the Double Relaxation.

In 1971, Fünfshilling, Lemaréchal and Cerf (10) reported that the ultrasonic relaxation of solutions of polyvinyl pyridine (P. V. Py.) in the megahertz range can be represented by the equation of double relaxation (10). For the explanation of their results, they assumed two kinds of segments of different length. According to them, the potential for the internal rotation is mostly determined by the configuration near the rotating bonds, and not by the length of the segment.

As has been already mentioned, Ludlow, Wyn-Jones and Rassing showed that in the solution of polystyrene in D. M. F., the ultrasonic relaxation was also represented by the equation of double relaxation (26). They ascribed this double relaxation to a three-state model. They assumed the transitions of three states I, II and III ;



According to them;

State I of lower energy which is made up of all the energies of the benzene rings which are atactic with respect to both neighbours.

State II is made up of the energies of all the remaining diads of benzene rings which are in closest position with respect to each other.

State III of highest energy is made up of the energies of all the triads with neighbouring benzene rings in the closest position with respect to each other.

Ono, Shintani, Yano and Wada (45) have proposed somewhat different mechanism

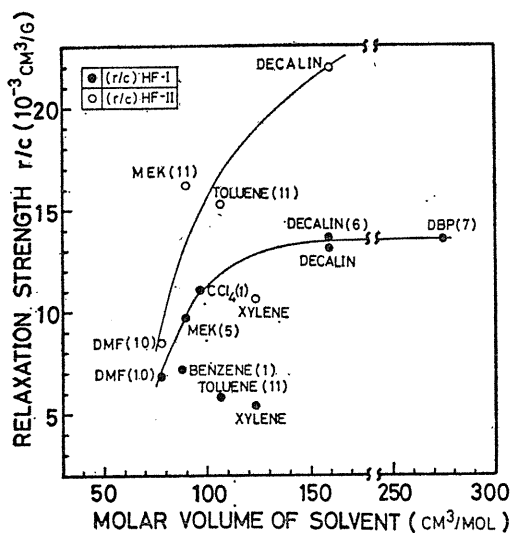


Fig. 19. Relaxation strength for the HF— I (dot) and the HF— II (circle) relaxations of polystyrene in various solvents plotted against the molar volume of the solvents. (K. Ono et al, (45))

for the ultrasonic relaxation of polystyrene solutions. They alleged that relaxation in megahertz range is essentially double and these two relaxations lie close together. The relaxation is, according to them, not thermal. The relaxation is ascribed to the volume change due to the internal rotation. The relaxation is, therefore, volume relaxation. The relation between the relaxation strength and the molar volume of the solvents given by them is reproduced in Fig. 19, which seems to support their assumption.

The plot of relaxation strength against the molar volume is also given in Fig. 20 for polyvinyl pyrrolidone as well as polystyrene, data of which were taken from the data shown in Table I. In this figure, no such systematic trend is observed. The result is unfavourable for the Ono's model since the molecular structure of P. V. P. is not so much different from that of polystyrene.

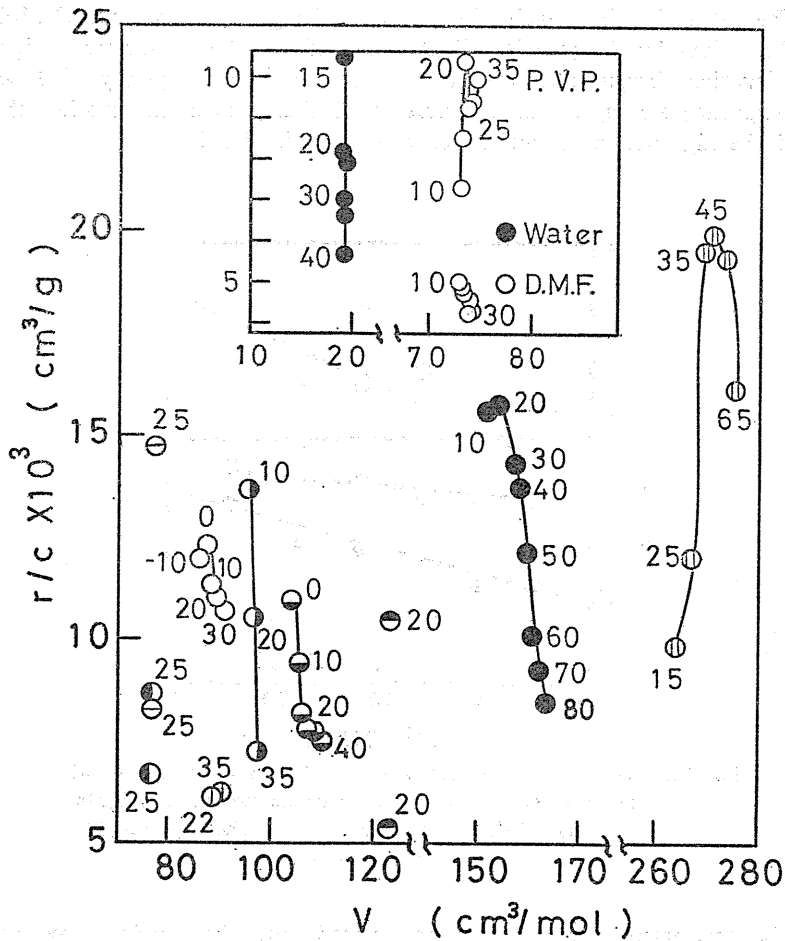


Fig. 20. Relation between relaxation strength and molar volume of solvent. (18)
(Polystyrene in various solvents and P. V. P. in aqueous solution and in D. M. F.)

4. 1. 3. Ultrasonic Relaxation in the KHz Range.

Ono, Shintani, Yano and Wada (45) have also suggested the existence of another relaxation in the kilohertz range in the polystyrene solutions from their measurements by the reverberation method. The strength of this relaxation is far greater than that of the relaxation due to the shear viscosity, and the relaxation time increases with the increases in the molecular weight. They explain the origin of this relaxation as the heat conduction between the molecular globes containing solvent molecules in them and the external solvent.

4. 1. 4. Ultrasonic Relaxation of Polystyrene of Low Molecular Weight.

As has already been mentioned, the ultrasonic relaxation found in the megahertz range for the solutions of polystyrene of molecular weight 2,100 and 4,000 is quite different from that of high molecular weight in its relaxation mechanism.

It must be noted here the following facts.

- (1). The relaxation frequencies lie in higher frequency range, *ca.* 20 MHz.
- (2). The relaxation frequencies slightly depend on the molecular weight. The relaxation frequencies are shifted to the high frequency side with the temperature rise, but their temperature change is much smaller than that of the high molecular weight polymers. (cf. Fig. 21)

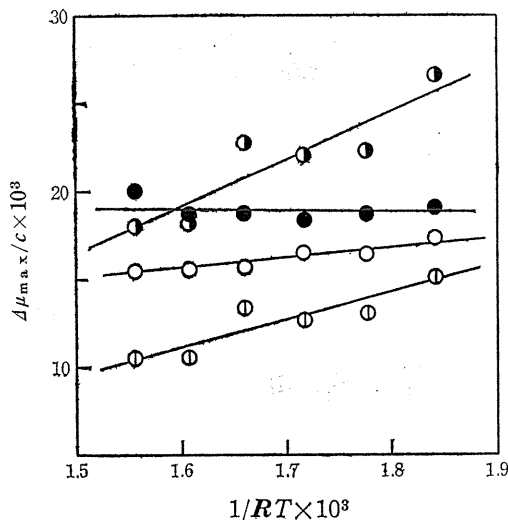


Fig. 21. Temperature dependence of relaxation strengths of the polymers per g/ml with various molecular weights.
Molecular Weight ●; 2,100, ○; 4,000, ⊙; 300,000
⊖; 2,000,000

- (3). The relaxation curve is completely fitted with the single relaxation equation.
- (4). The constant *A* in the relaxation equation is almost independent of molecular weight. (cf. Figs. 9, 10 and 11).

Since the temperature dependence of the relaxation frequency and the relaxation

strength of this relaxation are entirely different from those of the relaxation of polystyrene of higher molecular weight, it is natural to assume that the relaxation mechanism of the low molecular weight polystyrene is not the thermal relaxation due to the crank-shaft motion.

We suggest here that the ultrasonic relaxation of low molecular weight polystyrene is caused by the motions of end group of the molecules. (cf. Fig. 22)

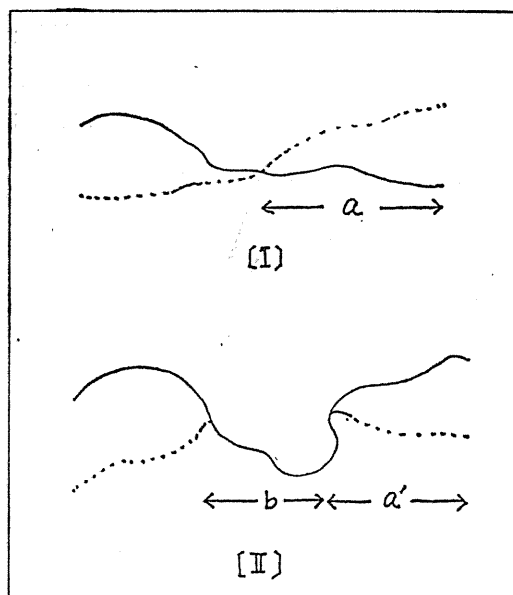


Fig. 22. Molecular motion of chain end.

The slight molecular weight dependence of the relaxation strength is explained as follows. When the molecular weight increases, the length of the vibrating end (a' in Fig. 22 (II)) is increased, and the relaxation frequency is shifted to the low frequency side. In this case, the remaining part is still not long enough to allow the crank-shaft type internal rotation in it.

There are a number of modes of the vibrational motion of the end groups, and only one mode of longest relaxation time is observed as the single relaxation. The relaxation strength of motion of this is 40 at 30°C and only 1% of that of polystyrene of molecular weight 300,000, which is 4.1×10^3 .

4. 2. Ultrasonic Relaxations in Solutions of Polyvinyl Acetate, Polyvinyl Propionate and Polyvinyl Butylate.

The effect of the length of side chain on the ultrasonic relaxation is examined from the data of polyvinyl acetate (P. V. Ac.), polyvinyl propionate (P. V. Pr.) and polyvinyl butylate (P. V. Bu.). (40, 41, 43). The available data are those of toluene solutions of P. V. Ac., P. V. Pr. and P. V. Bu. reported by us and acetone solutions of P. V. Ac. reported by Masuda, Ikeda and Ando (28). For the toluene solutions of P. V. Ac., P. V. Pr. and P. V. Bu., the measured frequency range was from 1 to

130 MHz. The plots of absorption parameter against frequency at various temperatures were well represented by the equation of double relaxation. In Fig. 23,

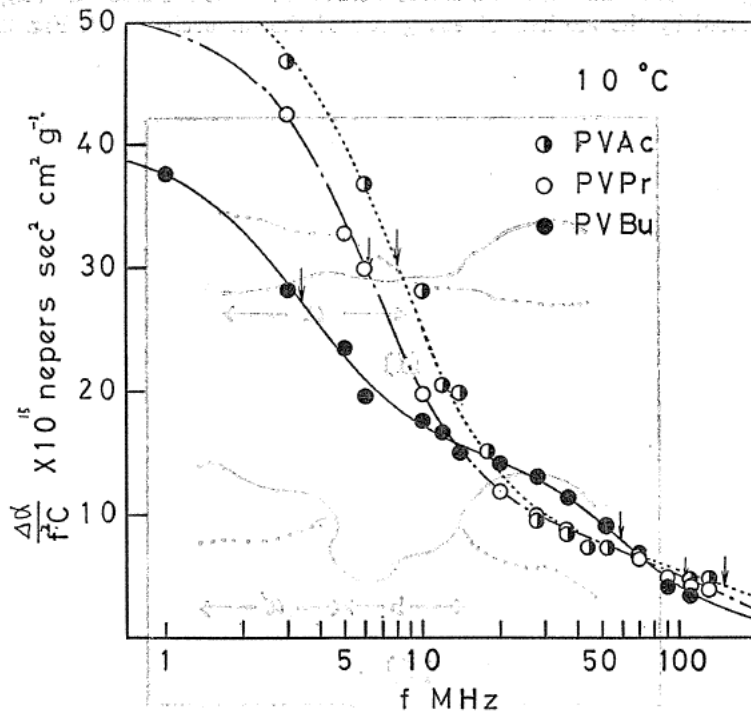


Fig. 23. Frequency dependence of ultrasonic absorption in P. V. Ac, P. V. Pr and P. V. Bu-toluene solutions at 10°C.

the experimental results at 10°C for P. V. Ac., P. V. Pr. and P. V. Bu. are shown, and in Fig. 24, the temperature change is shown for P. V. Bu.. The relaxation parameters obtained are summarized in Table 5, together with those obtained by Masuda, Ikeda and Ando (28). As is seen in Fig. 23, the relaxation frequencies, f_{r1} and f_{r2} , are both shifted to the low frequency side with the increase in the length of side chain.

The Arrhenius plots of f_{r1} and f_{r2} for P. V. Ac., P. V. Pr. and P. V. Bu. are shown in Fig. 25.

4. 2. 1. Effect of Side-chain-length on the Low Frequency Side Relaxation Frequency.

It is clearly seen in Figs. 23, 24 and 25, that the relaxation mechanism at lower frequency is entirely same, as that observed in the solutions of polystyrene. The relaxation strength and relaxation frequency lie in the same order of magnitude of polystyrene. The relaxation frequency is related to the moment of inertia of

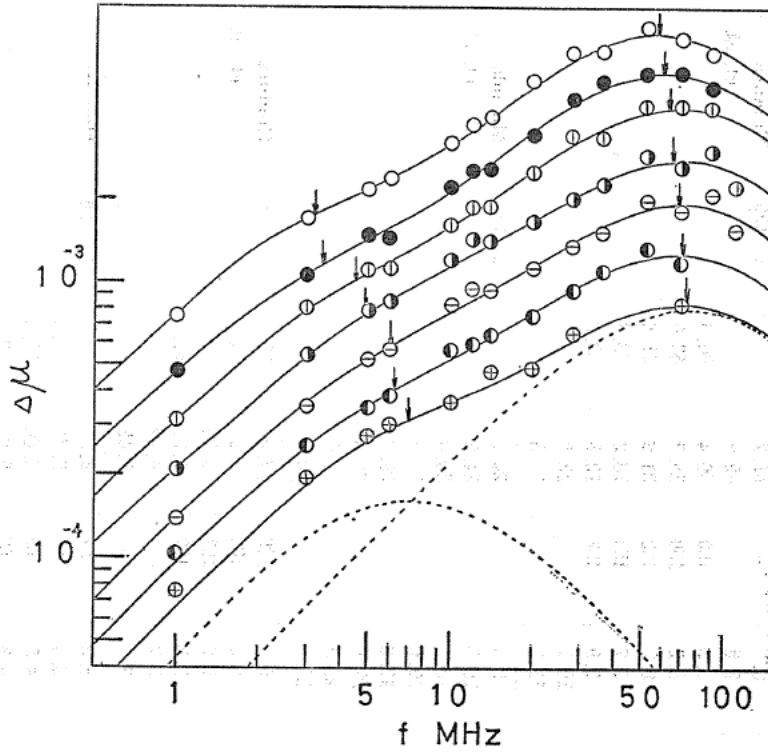


Fig. 24. Frequency dependence of absorption per unit wave length of P. V. Bu-toluene solutions at various temperatures.

Temperature ($^{\circ}\text{C}$) \circ ; 0, \bullet ; 10, $\text{\textcircled{v}}$; 20, $\text{\textcircled{h}}$; 30, $\text{\textcircled{/}}$; 40, $\text{\textcircled{+}}$; 50, $\text{\textcircled{x}}$; 60

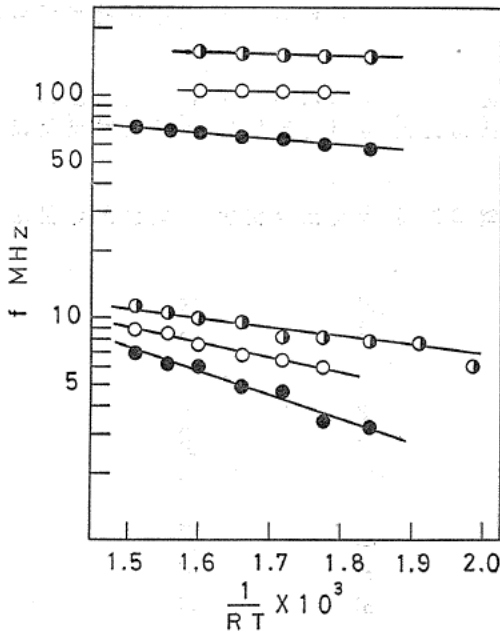


Fig. 25. Relation between f_{r1}, f_{r2} and $1/RT$.

\bullet ; P. V. Bu, \circ ; P. V. Pr, $\text{\textcircled{v}}$; P. V. Ac

Table 5. Relaxation Parameters of P. V. Ac, P. V. Pr and P. V. Bu.

Polymer	Solvent	Deg. Poly.	temp. C	A_1/C $\times 10^{15}$	A^2/C $\times 10^{15}$	B/C $\times 10^{15}$	f_{T_1} MHz	f_{T_2} MHz	μ_{1max}/C $\times 10^3$	μ_{2max}/C $\times 10^3$	frequency ranges	Ref.					
P. V. Ac	Toluene	2000	-20	117.3	—	4.2	6.9	—	61.7	—	1—130	Nomura et. al.					
			-10	79.7	—	4.6	7.8	—	45.9	—							
			0	64.5	6.2	0.7	7.9	150	36.4	66.3							
			10	46.5	6.2	0.9	8.2	150	26.3	63.0							
			20	40.0	6.1	0.9	8.2	152	21.9	61.8							
			30	29.1	5.7	0.9	9.7	154	18.2	56.8							
			40	20.5	5.4	0.9	9.9	157	12.6	52.3							
			50	19.9	—	4.2	10.7	—	12.8	—							
			60	15.5	—	3.7	11.5	—	10.3	—							
			P. V. Pr	Toluene	2000	0	30.5	—	3.4	12.4			—	24.0	—	5—75	Masuda et. al.
						5	25.2	—	4.0	15.3			—	24.2	—		
						7	26.8	—	3.2	18.1			—	30.0	—		
10	22.0	—				3.8	19.0	—	25.6	—							
12	24.8	—				3.6	19.6	—	29.8	—							
15	22.2	—				2.2	22.6	—	30.4	—							
17	20.9	—				1.2	23.3	—	33.0	—							
20	19.0	—				3.0	26.9	—	30.4	—							
P. V. Bu	Toluene	2000				0	41.7	7.7	0.8	6.2	105	17.8	55.7	1—130	Nomura et. al.		
						10	32.6	7.7	0.8	6.5	106	14.1	54.5				
						20	20.6	7.7	1.0	6.9	107	9.20	53.1				
						30	20.6	7.7	1.0	7.8	107	7.58	51.3				
			40	15.6	—	8.1	8.7	—	5.12	—							
			50	9.8	—	8.4	9.0	—	3.42	—							
			60	6.6	—	—	—	—	—	—							
			P. V. Bu	Toluene	2000	0	30.5	15.7	0.3	3.2	57	6.97	63.9			1—130	Nomura et. al.
						10	24.3	15.0	0.3	3.4	60	5.71	61.9				
						20	18.2	12.0	0.4	4.5	63	5.46	53.1				
						30	16.1	11.4	0.6	4.8	65	5.00	48.0				
						40	15.8	9.7	0.6	6.0	68	5.92	41.0				
50	13.2	7.6				0.7	6.2	70	4.93	32.2							
60	11.7	5.6				0.9	7.0	72	4.76	23.3							

local internal rotation in the relation

$$f_r \propto \frac{1}{I^{1/2}} \quad (46)$$

Since $I = mr^2$ (m the mass, r the length), and f_r is related to the length of side chain L as

$$f_r \propto \frac{1}{L} \quad (47)$$

In Fig. 26, the relaxation frequencies f_{r1} of P. V. Ac., P. V. Pr. and P. V. Bu. given in Fig. 23 are plotted against the carbon number of side chain $-\text{CH}_2-\text{CH}_2-$. The plot seems to support the present postulation that the low frequency side relaxation is thermal relaxation due to the crank-shaft motion in the back-bone chains.

The relaxation parameters calculated on the basis of the two-state model are shown in Table 6. As is seen in the table, ΔH_0 decreases slightly with the increase in length of side chain, and ΔH_{21} increases with it. These results also support the present postulation.

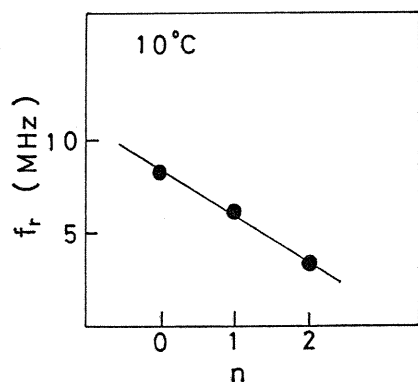


Fig. 26. Relation between f_{r1} and length of side chain.

Table 6. Activation Energies of P. V. Ac, P. V. Pr and P. V. Bu.

Polymer	Solvent	ΔH_0^1	ΔH_{21}^1	ΔH_{app}^I
		Kcal/mol	Kcal/mol	Kcal/mol
P. V. Ac.	Toluene	1.36	1.0	0.2
	Acetone	1.50	5.67	—
P. V. Pr.	Toluene	1.30	1.28	0.2
P. V. Bu.	Toluene	1.28	2.24	0.7

4. 2. 2. Mechanism of the High-Frequency Side Relaxation.

As is clearly seen in Fig. 23 and Table 5, the toluene solutions of P. V. Ac., P. V. Pr. and P. V. Bu. show the second relaxation in the range of 150 MHz. The relaxation frequencies f_{r2} are shifted to low frequency side with the increase in the length of side chains. The relaxation frequency of P. V. Bu. is about a half of P. V. Ac. Table 6 shows that the apparent activation energies of f_{r2} are about one fifth of that of first relaxation at lower frequency.

Fünfschilling, Lemaréchal and Cerf (10) have suggested that these two relaxations are due to two local internal rotations in the back-bone chains, one is of wide range, and the other is included in the former.

It seems, however, more natural to assume that these high-frequency side relaxations are due to the motions of side chains themselves.

4. 3. Ultrasonic Relaxation in Aqueous Solutions of Polyvinyl Pyrrolidone.

Polyvinyl Pyrrolidone (P. V. P.) is water-soluble polymer having 2-pyrrolidone

Table 7. Relaxation Parameters of P. V. P. in water and D. M. F.

Solvent	M.W. $\times 10^4$	temp. $^{\circ}\text{C}$	A_1/C $\times 10^{15}$	A_2/C $\times 10^{15}$	B/C $\times 10^{15}$	f_{r_1} MHz	f_{r_2} MHz	$\mu_{1\max}/C$ $\times 10^{-3}$	$\mu_{2\max}/C$ $\times 10^{-3}$	frequency ranges	Ref.			
Water	1.0	10	20.8		2.1	8.1		12.4		5—130	Kato et. al			
		15	17.2		1.8	9.0		11.5						
		20	12.6		1.3	11.7		11.1						
		25	11.0		1.2 ₅	11.7		9.8						
		30	10.6		1.1	10.4		8.4						
		35	10.0		1.0	10.1		7.8						
		40	9.3		0.9	10.6		7.6						
		2.25	10	22.0		2.1	8.3		13.43					
		2.25	15	17.1		1.8	9.2		11.72					
			20	14.6		1.5	9.6		10.54					
			25	14.5		1.5	8.4		9.25					
			30	12.3 ₇		1.2	8.0		7.56					
			35	14.0 ₇		1.5	6.7		7.25					
			40	11.6		1.0	8.1		7.27					
			4.0	4.0	10	23.36		2.10	8.1			13.92		
					15	20.12		1.81	8.5			12.73		
	20	16.77				1.47	8.9		11.22					
	25	15.56				1.47	8.2		9.68					
	30	14.07				1.21	8.4		9.03					
	35	15.05				1.47	6.8		7.87					
	40	13.40				1.04	7.6		7.85					
	36.0	36.0			10	27.0		1.9	10.0			19.9		
			15	21.7		1.7	10.0		16.5					
			20	16.8		1.7	10.1		12.8					
25			17.7		1.4	9.3		12.5						
30			18.0		1.3	8.1		11.1						
35			16.9		1.0	8.0		10.4						
40			16.5		0.9	7.0		8.9						
D. M. F			36.0	10	11.55	2.46	1.18	9	61	7.94	11.45	4.2—130	Kato et. al.	
	15	10.14		2.90	1.03	10	61	7.64	13.35					
	20	10.05		3.24	0.89	10	68	7.47	16.37					
	25	9.16		3.24	0.89	10	61	6.72	14.50					
	30	8.26		3.02	0.78	12	68	7.18	14.85					
	35	8.26		3.35	0.54	11.5	65	6.79	15.56					

in its side chain. Since it has the side chains of -N-C- , it is considered as a model substance of protein. The determination of amount of hydration of this polymer has been reported (32). The amount of hydration decreases with the temperature rise, and above 45-50°C, the dehydrated molecules in water behave like molecules of other synthetic polymers in organic solvents (32). The experimental results of measurements of ultrasonic absorption in the aqueous solutions of P. V. P. and solutions in D. M. F. are summarized in Table 7 (16, 18).

In Figs. 27, 28 and 29, the absorption parameters, $\Delta\alpha/f^2$, are plotted against the frequency for P. V. P. of molecular weight 1.0×10^4 , 2.25×10^4 , 4.0×10^4 and 36.0×10^4 in the frequency range from 5 to 130 MHz at the temperatures 10°- 40°C. Figs. 28 and 29 show that these plots obey the single relaxation equation. The temperature dependence of the relaxation parameters, A , B and f_r is shown in Figs. 30 and 31.

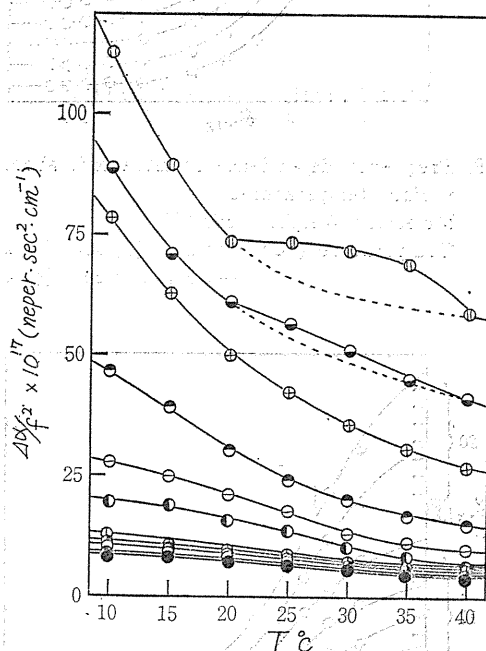


Fig. 27. Temperature dependence of ultrasonic absorption at various frequencies.

Molecular Weight; 360,000.

Frequency (MHz) \oplus ; 5, \ominus ; 7, \oplus ; 9, \ominus ; 15, $\omin�$; 21, $\omin�$; 30, \oplus ; 50, $\omin�$; 70, \circ ; 90, \oplus ; 110, $\omin�$; 130

As is clearly seen in Figs. 28 and 29, the profiles of single relaxation curves of aqueous solutions of P. V. P. are not changed by the dehydration, which is accomplished at 25°C.

The ultrasonic relaxation in the aqueous solutions of P. V. P. is probably due to the local hindered rotation of back-bone chains as in the case of polystyrene.

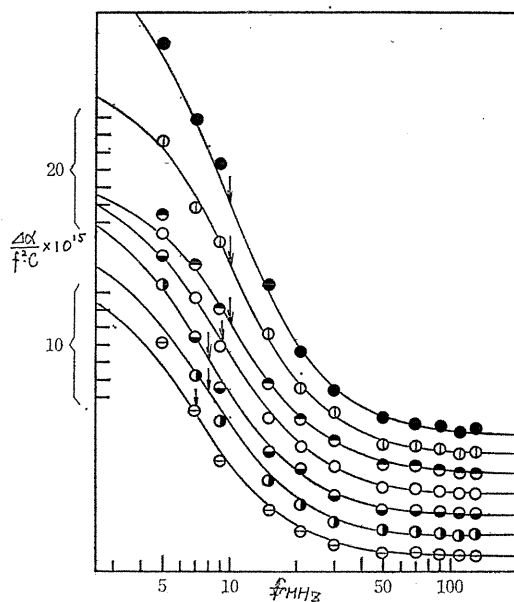


Fig. 28. Frequency dependence of ultrasonic absorption at various temperatures.

Molecular Weight; 360,000

Temperature ($^{\circ}\text{C}$) ●; 10, ⊕; 15, ⊖; 20, ○; 25,
 ⊙; 30, ⊗; 35, ⊘; 40

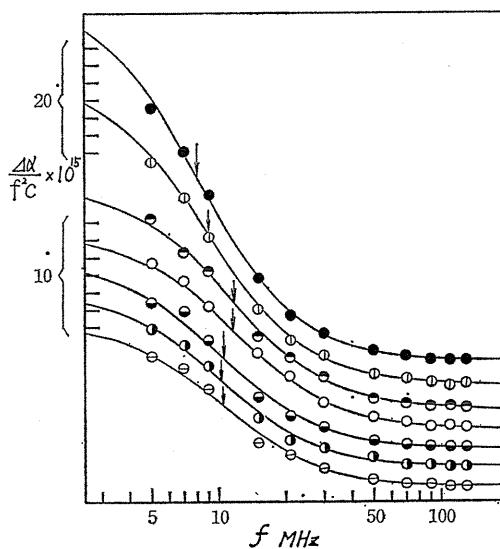


Fig. 29. Frequency dependence of ultrasonic absorption at various temperatures.

Molecular Weight; 10,000

Temperature ($^{\circ}\text{C}$) ●; 10, ⊕; 15, ⊖; 20, ○; 25,
 ⊙; 30, ⊗; 35, ⊘; 40

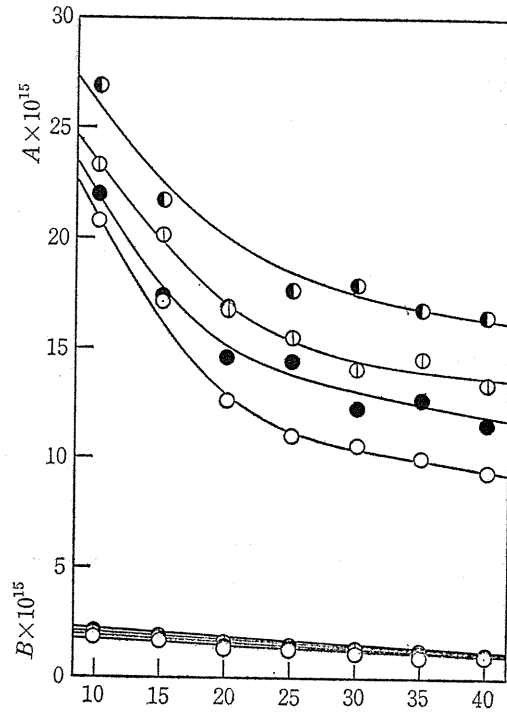


Fig. 30. Variation of relaxation parameters A and B with temperature.
 Molecular Weight \bullet ; 360,000, \circ ; 40,000,
 \bullet ; 24,500, \circ ; 10,000

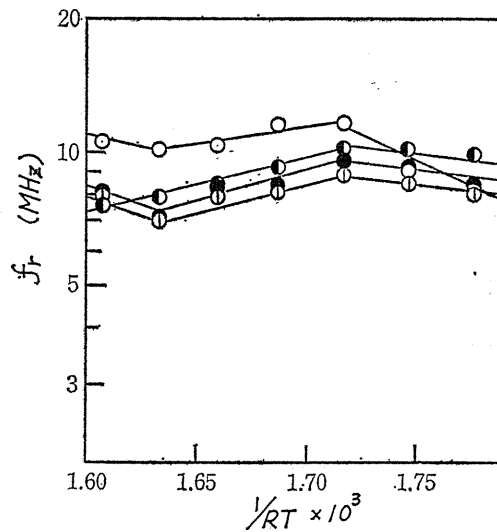


Fig. 31. Variation of relaxation frequency with reciprocal temperature.
 Molecular Weight \bullet ; 360,000, \circ ; 40,000,
 \bullet ; 24,500, \circ ; 10,000

The effect of hydration water on the relaxation curves is seen clearly in Fig. 27, where the absorption parameter $\Delta\alpha/f^2$ is plotted against temperature. In the figure, upper two curves show irregular shoulders, which give no significant effect on the profile of relaxation curve as a whole.

The loss of hydration water is considered to cause some change in the molecular conformation like a phase change. The effect of this conformation change on the relaxation is significant in the low frequency range below a few megahertz and this effect increases with the increase in the molecular weight.

The effect of loss of hydration water also appears in ΔH_{21} , which changes significantly at the temperature of dehydration. Below the dehydration temperature, ΔH_{21} is related to the interaction between the hydrated water and the surrounding water, whereas above 25°C, it is related to the interaction between unhydrated segments and the surrounding water. (Table 8)

Table 8. Activation Energies of P. V. P. in Aqueous Solutions.

M. W.	ΔH_{21} (Kcal/mol)		ΔH_0 (Kcal/mol)	
	10°—20°	35°—40°	10°—20°	35°—40°
10,000	4.3	4	0.7	0.7
24,500	1.4	4	0.7	0.7
40,000	1.4	4	0.7	0.7
360,000	1.4	—	0.7	0.7

In Figs. 32 and 33, the ultrasonic relaxation of P. V. P. of molecular weight

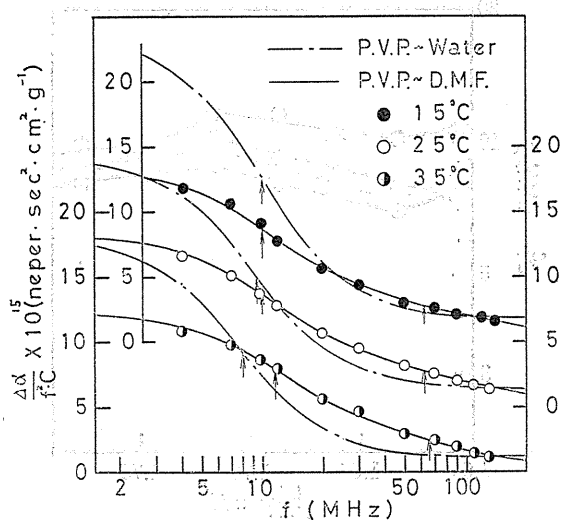


Fig. 32. Frequency dependence of ultrasonic absorption at various temperatures.

Molecular Weight; 360,000

— · — · — · ; P. V. P. - Water — ; P. V. P. - D. M. F.

Temperature (°C) ●; 15, ○; 25, ◐; 35

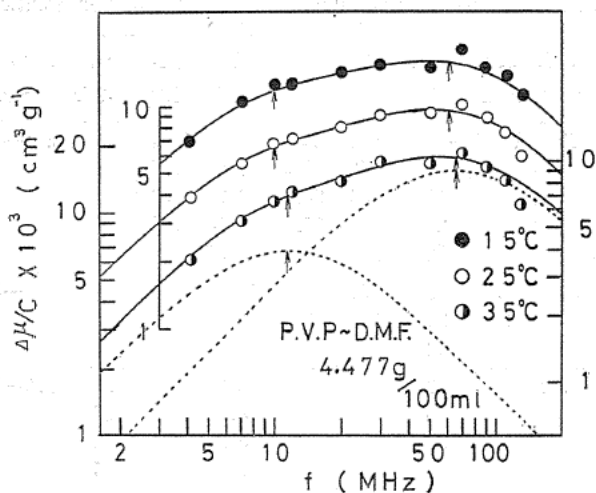


Fig. 33. Excess absorption per wave length for P. V. P. in D. M. F. solution.
Temperature ($^{\circ}\text{C}$) \bullet ; 15, \circ ; 25, \circ ; 35

360,000 in the D. M. F. solutions is shown. It is noted that in the D. M. F. solutions, the relaxation of P. V. P. is double. The relaxation parameters are listed in Table 7. The relaxation frequency of the low frequency side, f_{r1} , is not so much changed between in water and D. M. F..

In general, the first relaxation frequencies of lower frequency side of the vinyl-polymer are almost independent of the solvents used, whereas those of higher frequency side are significantly affected by the solvents. In Table 9, various parameters in relaxation processes of P. V. P. -D. M. F. system calculated on the basis of the two-state model are shown.

Table 9. Activation Energies of P. V. P. in D. M. F.

	ΔH_0 Kcal/mol	ΔH_{21} Kcal/mol
f_{r1}	1.15	1.50
f_{r2}	2.90	0.49

4. 4. Ultrasonic Relaxation in Other Vinyl-Polymer Solutions.

The ultrasonic relaxations are also observed in the following polymer solutions.

- I polymethylmethacrylate - toluene (35, 30)
- II polyvinylpyridine - chloroform (9)
- III polyvinylpyridine - dioxane (8)
- IV polymethacrylic acid - acetone (29)
- V polymethacrylic acid - toluene (15)
- VI polymethacrylic acid - dichloroethane (15)

Among them, the systems I, IV, V, and VI exhibit the single relaxation, whereas II, III, the double relaxation.

In Fig. 34, the relaxation curves of the system P. V. Py. - chloroform are shown, and in Table 10 the relaxation parameters of these solutions are summarized.

Table 10. Relaxation Parameters of Various Polymer Solutions.

Polymer	Solvent	M. W. $\times 10^3$	conc. g/dl	temp. °C	A	B	f_r MHz	μ_{\max} $\times 10^{-3}$	f_{r_2} MHz	frequency ranges	Ref.						
P. M. M. A	Toluene	100	2.912	-10	586	24.8	2.65	1.14		3 — 60	Nomura. et. al.						
				0	363	22.4	3.98	1.03									
				10	304	20.1	4.70	1.00									
				20	259	17.4	6.14	1.10									
				30	253	15.8	6.86	1.12									
	Benzene	3.1	4	7			3.8		25	1.6—100	Fünfschilling et. al.						
				20			4.5	25									
				30			4.5	20									
	P. V. Py	Dioxane	28	3	15			1.8		20	1.6—100	Fünfschilling et. al.					
					25			2.2	20								
35							3	20									
45							4	20									
P. M. A	Acetone	56	5.70	-10	144	11	16.1	15.3		7 — 85	Masuda et. al.						
				5	104	12	18.3	1.73									
				5	105	9	21.7	1.42									
				15	63	11	26.6	1.01									
				20	71	3	27.4	1.15									
				25	62	9	32.9	1.19									
				Dichloroethane	88	4.00	1.5	-10	101			6	15.3	1.02		7 — 85	Masuda et. al.
								-5	79			0	25.8	1.33			
								1	74			1	27.3	1.28			
								5	73			4	24.9	1.14			
	10	70	12					17.6	0.79								
	15	72	15					19.1	0.83								
	17	112	19					16.6	1.37								
	20	78	18					15.1	0.70								
	25	63	20					18.9	0.70								
	Toluene	108	3.00					3.0	10	6914	16	1		14	7 — 65		
				20	507	0	2		33								
				25	521	8	3		40								
				30	119	0	7		40								

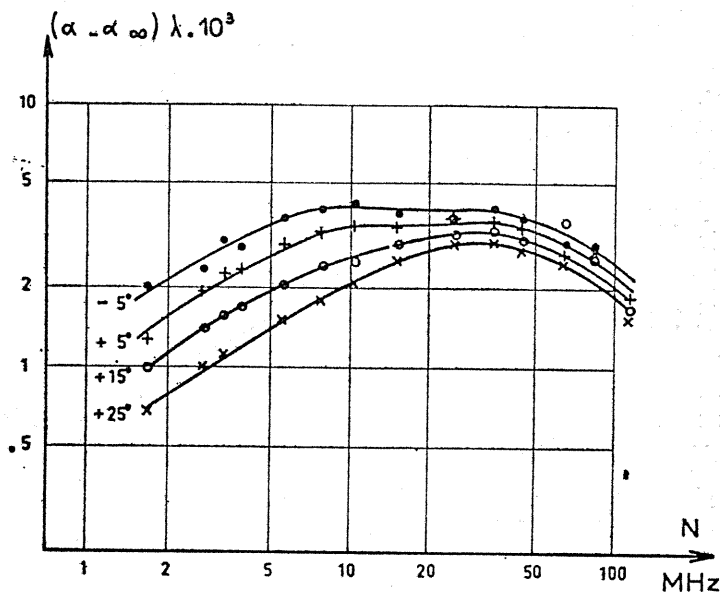


Fig. 34. Ultrasonic absorption per wave length at four temperatures in chloroform solutions of P. V. Py.
 Concentration; 3×10^{-2} (g/ml)
 Temperature ($^{\circ}\text{C}$) \bullet ; -5 , $+$; 5 , \circ ; 15 , \times ; 25
 (O. Fünfschilling et al., (9))

4. 5. Ultrasonic Absorption in Solutions of Miscellaneous Polymers.

4. 5. 1. Ultrasonic Absorption in Solutions of Polycarbonate. (17)

For the purposes of examining the effect of back-bone structure of polymer molecules on the local motions of segments in the back-bone chain, the ultrasonic absorptions in the solutions of polycarbonate such as poly-4-4-dihydroxydiphenyl carbonate were studied.

4. 5. 1. 1. Dioxane Solutions.

The ultrasonic absorption coefficient of pure dioxane increases with the temperature rise, and absorption parameter α/f^2 is independent of the frequency. The ultrasonic relaxation does not therefore exist in the solvent in this frequency range.

In Fig. 35, the frequency dependence of ultrasonic absorption in dioxane solution of P.C. at 25°C is shown as an illustrative example. In the figure, the plot deviates from the single relaxation curve which is shown by the dotted line.

The experimental values can be fitted by an equation of double relaxation which is shown in the figure as the solid line. In Fig. 36, the excess absorption per wave length, $\Delta\mu/c$ is plotted against the frequency at various temperatures. In this figure, upper four curves are shifted upward arbitrarily. In Table 11, the relaxation parameters in the double relaxation equation are summarized.

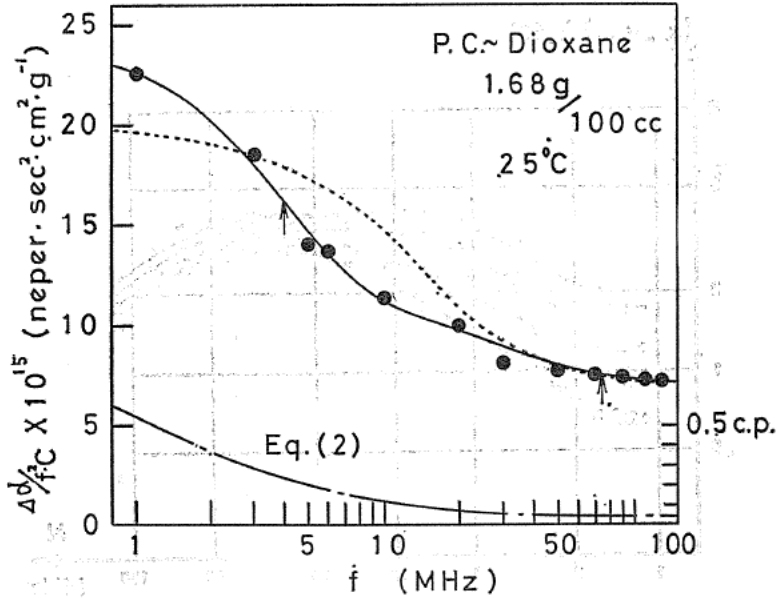


Fig. 35. Frequency dependence of ultrasonic absorption of polycarbonate in dioxane at 25°C.

.....; single relaxation process
 ———; double relaxation process

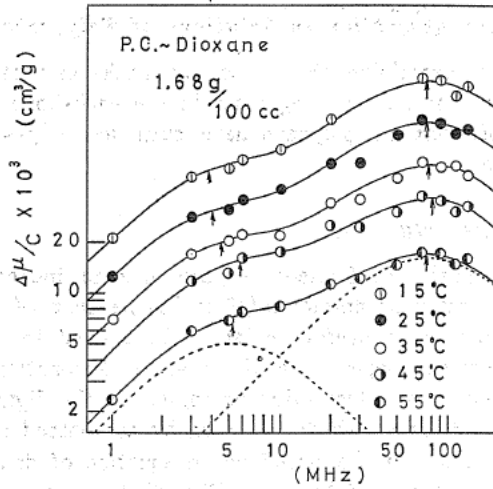


Fig. 36. Excess absorption per wave length for polycarbonate in dioxane solutions.

Temperature (°C) ○; 15, ●; 25, ○; 35, ●; 45, ●; 55

Table 11. Relaxation Parameters for P. C. in Dioxane Solutions.

	$A_1/C \times 10^{15}$ neper·sec ² cm ² ·g ⁻¹	$A_2/C \times 10^{15}$ neper·sec ² cm ² ·g ⁻¹	$B/C \times 10^{15}$ neper·sec ² cm ² ·g ⁻¹	f_{r1} MHz	f_{r2} MHz	$\mu_1/C \times 10^3$ cm ³ ·g ⁻¹	$\mu_2/C \times 10^3$ cm ³ ·g ⁻¹
1.5	13.3	3.7	6.0	3.8	7.4	3.54	19.2
2.5	14.3	3.7	5.5	4.0	7.4	3.94	18.8
3.5	15.2	3.7	5.5	4.5	7.6	4.47	18.4
4.5	16.6	3.7	5.9	5.7	8.0	5.96	18.7
5.5	16.4	3.6	5.5	5.2	7.4	5.10	16.4

4.5.1.2. Chloroform Solutions.

In Fig. 37, the frequency dependence of ultrasonic absorption parameter for

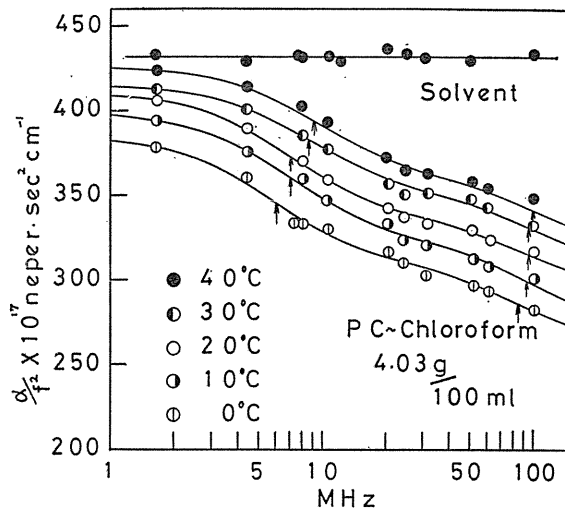


Fig. 37. Frequency dependence of ultrasonic absorption of polycarbonate in chloroform.

Temperature (°C) ○; 0, ◐; 10, ○; 20, ◑; 30, ●; 40

chloroform solutions of P. C. is shown. As is seen in the figure, the relaxation curves are of double relaxation. No ultrasonic relaxation is observed in pure chloroform, although the value of α/f^2 is rather high. In chloroform solutions, the absorption coefficient of the solution is smaller than that of pure solvent, and the excess absorption, $\Delta\alpha = \alpha - \alpha_0$ is negative. In Fig. 37, the ordinate is the absorption parameter of solution itself. In Table 12, the relaxation parameters in the double relaxation equation are summarized.

In Table 13, the apparent activation energies in dioxane and chloroform obtained from the temperature change of relaxation frequencies are listed.

Table 12. Relaxation Parameters for P. C. in Chloroform Solutions.

	$A/C \times 10^{15}$ neper·sec ² cm ² ·g ⁻¹	$A_2/C \times 10^{15}$ neper·sec ² cm ² ·g ⁻¹	$B/C \times 10^{15}$ neper·sec ² cm ² ·g ⁻¹	f_{r_1} MHz	f_{r_2} MHz	$\mu_1/C \times 10^3$ cm ³ ·g ⁻¹	$\mu_2/C \times 10^3$ cm ³ ·g ⁻¹
0	18.6	11.4	62.6	6.0	8.4	5.97	51.2
10	18.4	12.4	68.0	7.0	9.2	6.66	59.2
20	18.1	10.9	72.7	7.0	9.4	6.35	51.4
30	15.4	10.4	76.9	8.5	9.4	6.33	47.4
40	15.9	11.9	77.9	9.0	10.0	6.66	55.5

Table 13. Apparent Activation Energies of Polycarbonate in Dioxane and Chloroform.

Solvent	ΔH_{app1} Kcal/mol	ΔH_{app2} Kcal/mol
Dioxane	1.85±0.33	0.15±0.14
Chloroform	1.70±0.17	0.63±0.09

The relaxation in lower frequency range 1~10 MHz, is ascribed to the thermal relaxation caused by the hindered rotation of local groups in the back-bone chains.

Since it is believed that the back-bone chain of polycarbonate molecules is semi-flexible, the crank-shaft motion of a few segments is not allowed. Therefore, the rotational motions considered here are co-operative motions of several groups. This assumption may be supported by the facts that the relaxation frequency is not so significantly changed by the change in the structure of the back-bone chain, and the apparent activation enthalpy is not so much different from that of vinyl polymers.

Since the molecules of polycarbonate do not have long side chains as the vinyl polymer, the relaxation in the higher frequency range can not be ascribed to the motions of side chains. The model proposed by Fünfshilling, Lemaréchal and Cerf for vinyl polymer (10) is suggestive as a cause of the low frequency relaxation. According to them, there exist two different modes of relaxation motion, the motion of one of which is included in that of the other.

As mentioned above, the absorption coefficient of solvent is larger than that of the solution. As reported by Tondre and Cerf (55), the system P. M. M. A. - benzene shows similar behaviour. Tondre and Cerf have ascribed these phenomena to the interaction between the vibration relaxation of benzene molecules and intramolecular vibrations of polymer molecules.

The decrease of ultrasonic absorption with the increase in the concentration of P. C. in the chloroform solutions can be also ascribed to the solvent-solute interaction. In Raman spectra of chloroform solution of P. C., the intensities of lines 367 cm⁻¹ and 364.2 cm⁻¹ are changed significantly with the increase in the concentration of P. C. Teramachi, Takahashi and Kagawa (54) have reported that the partial molar entropy of P. C. in chloroform is largely negative. Reever and Schneider (50)

have concluded from the results of N. M. R. study that a π -complex is formed between hydrogen atom in chloroform molecule and benzene ring in the P. C. All these results support the presence of intense solute-solvent interaction in the system P. C. - chloroform.

Liquid chloroform exhibits the ultrasonic relaxation (7) which is ascribed to the vibration relaxation. The absorption observed in our experiments is its tail of the low frequency side. When the solute, P. C., is dissolved into the solvent, the strong interaction between the solvent and solute destructs the mechanism of vibrational relaxation of surrounding solvent molecules, and pushes down the back ground absorption to far lower side. And the thermal relaxation due to the local rotation of small group in the back-bone chain reveals which gives the single relaxation curve. The decrease in the value of α/f^2 in P. C. - chloroform solutions when vibrations, $\nu_6=262\text{ cm}^{-1}$, $\nu_3=365.9\text{ cm}^{-1}$, and $\nu_2=668.3\text{ cm}^{-1}$ are frozen, was calculated according to Lamb's theory (1). The result is shown in Fig. 38 by a broken

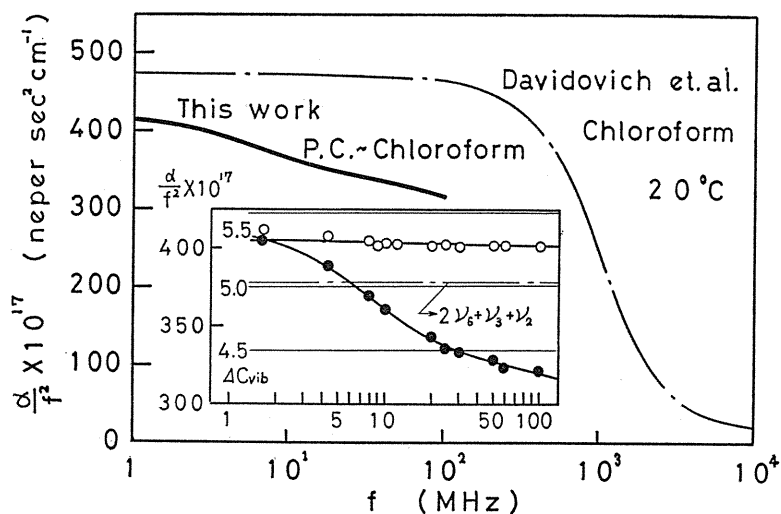


Fig. 38. Estimation of vibrational relaxation

line. The decrease is not sufficient to account for the present results. In this figure, the results of Davidovich, Ivanov, Makhkamov, Pulatova, Khabibullaev, Khalilulin, and Sharipov (7) are also shown.

4. 5. 2. Aqueous Solutions of Polyethylene Glycol.

The measurements of ultrasonic absorptions in aqueous solutions of polyethylene glycol were first reported by Hammes and Lewis (12), and later by Kessler, O'Brien and Dunn (20), who covered the frequency range from 1.5 MHz to 163 MHz.

The absorption coefficient changes linearly with respect to the concentration up to 20 g/100 ml. The samples of polyethylene glycol of molecular weight 4,500 and 20,000 gave identical relaxation time (cf. Fig. 39).

Kessler, O'Brien and Dunn have tried to explain these results on the basis of Zimm's theory. The relaxation mechanism of polyethylene glycol solutions seems

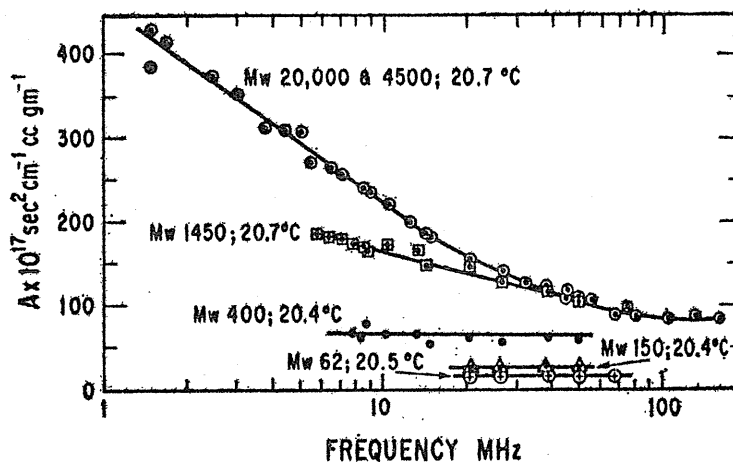


Fig. 39. Ultrasonic absorption of polyethylene glycol in aqueous solutions.

$$A = \Delta\alpha/f^2c \quad (\text{L. W. Kessler et al. (20)})$$

quite different from that of polyvinyl-type polymers, and it is rather shear-viscositic.

4. 5. 3. Dextran and Cellulose Derivatives.

The ultrasonic absorptions in aqueous solutions of dextran were first reported by Hawley and Dunn (13). According to them, the absorption parameter, $\Delta\alpha/f^2$,

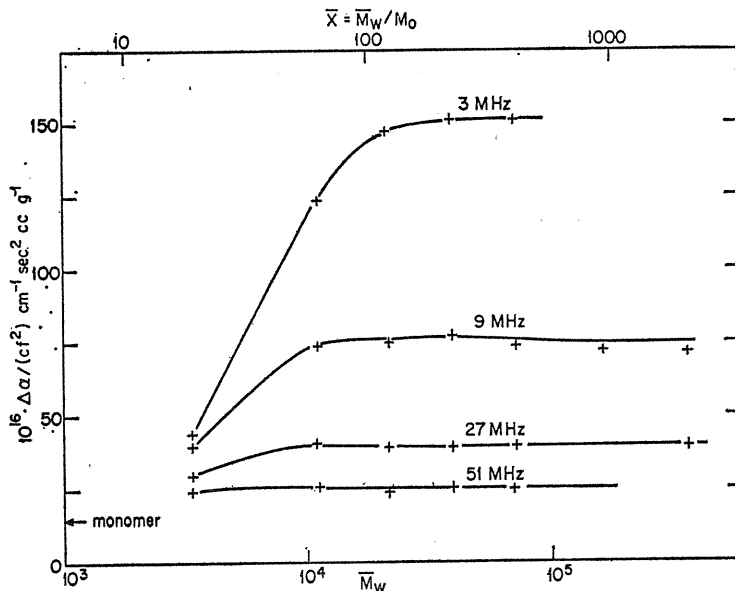


Fig. 40. $\Delta\alpha/f^2c$ as a function of weight average molecular weight at four frequencies at 20°C.

The average degree of polymerization \bar{x} is denoted on the upper-side abscissa. (S. A. Hawley and F. Dunn, (13))

was independent of the molecular weight above 1.0×10^4 (cf. Fig. 40). The experimental results obtained by us at the temperatures $5^\circ \sim 50^\circ\text{C}$ are shown in Fig. 41

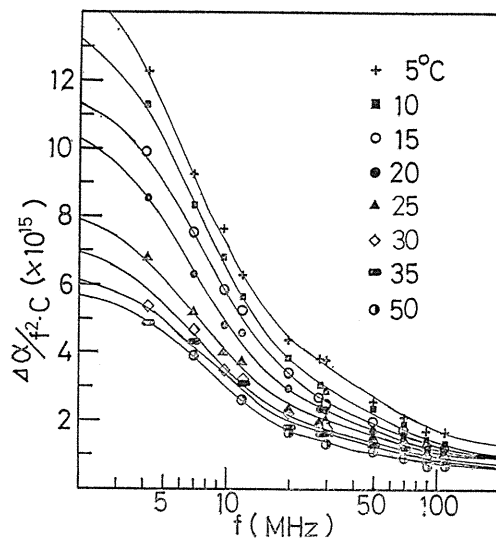


Fig. 41. Frequency dependence of ultrasonic absorption of dextran in aqueous solutions at various temperatures.

As is seen in the figure, a relaxation process is found in the megahertz range, which is not represented by a single relaxation equation.

In Fig. 42, the experimental results of solutions of cellulose triacetate dissolved in cyclohexanone (19) are shown, in which the results of dextran are also shown for

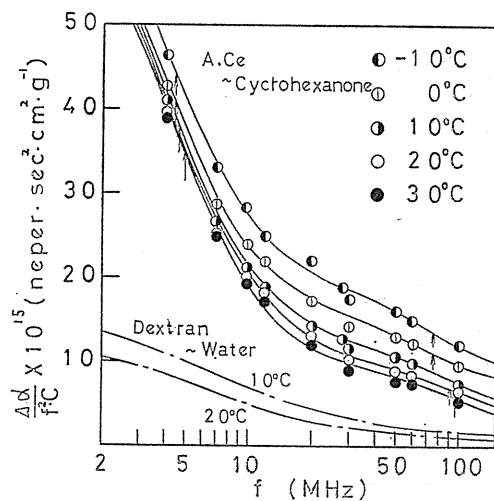


Fig. 42. Frequency dependence of ultrasonic absorption of cellulose acetate in cyclohexanone solutions.

comparison. In the Figs. 41 and 42, it is clearly seen that relaxation processes are present in the range from 70 to 100 MHz.

Dextran and cellulose acetate are semi-flexible polymers, and their ultrasonic relaxation behaviour is similar to that of polyethylene glycol system reported by Kessler and O'Brien and Dunn shown in 5.2. But in the cases of dextran-water and cellulose acetate-cyclohexanone systems the contributions of shear viscosity to the ultrasonic absorption estimated from the Zimm's theory are negligibly small.

4. 6. Abnormal Behaviour of Ultrasonic Relaxation caused by Changes in Conformation of Polymer Molecules.

The ultrasonic absorption caused by the helix-coil transition has already been reported in aqueous solutions of proteins and polyamino acids.

In the polystyrene-decalin system, abnormal solution behaviour at 70°C has been reported. Reiss and Benoit (51) have reported the abnormal behaviour in the second virial coefficient and radius of gyration obtained from the light-scattering measurements in this system. Similar phenomena were reported by several authors; Schmidt and Kovacs (52) in the measurements of specific volumes, Krigbaum, Mark, and Pritchard (21) and Okano (48) in the limiting viscosity number, Lee and Ullmann (24) in the high resolution N. M. R., and Wada and his coworkers in the compressibilities (57).

In Fig. 43, the absorption parameter $\Delta\alpha/f^2$, is plotted against frequency for the polystyrene-decaline system. In the figure, the curves of 10°~40°C are represented

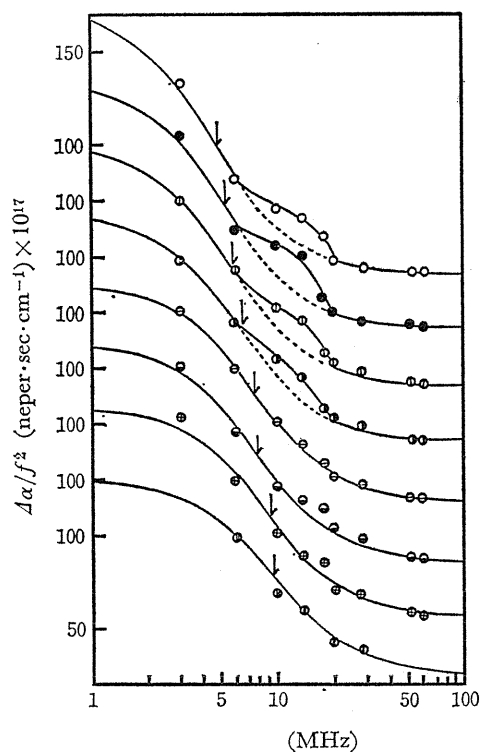


Fig. 43. Frequency dependence of polystyrene in decaline solution at various temperatures.

Temperature (°C)

- ⊕; 10, ⊗; 20, ⊙; 30, ⊖; 40,
●; 50, ⊚; 60, ⊛; 70, ○; 80

by the single relaxation equations. The curves of 50°~80°C deviate, however, from the single relaxation curves. In Fig. 44, the temperature change of the deviation from the single relaxation curves, $\Delta\alpha'/f^2$ is shown and the frequency dependence of the maximum value, $\Delta\alpha'_{\max}/f^2$ is illustrated (38).

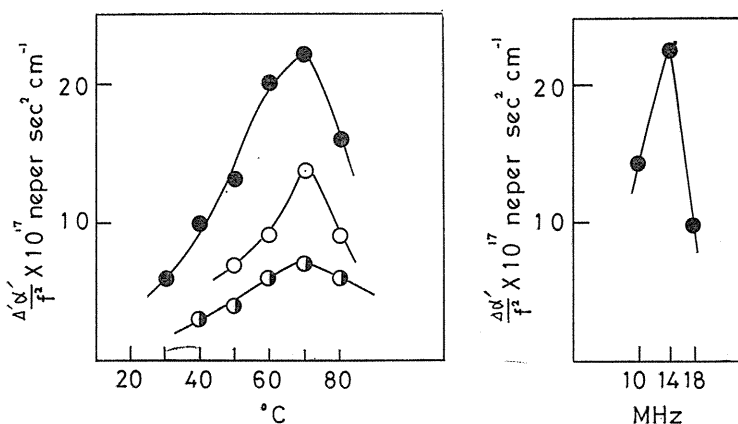


Fig. 44. Temperature dependence of abnormal absorption.
Frequency; (●); 10 MHz, (●); 14 MHz, (○); 18 MHz

As shown in 4.3., the aqueous solutions of polyvinylpyrrolidone show similar behaviour at the dehydration temperature. In Fig. 45, the temperature change of deviation from a single relaxation curve is shown for the polyvinylpyrrolidone - water system. Some abnormal behaviour is also found in the dielectric relaxation in this system (16).

It is well known that the ultrasonic absorption increases abnormally in the vicinity of the critical point and of some transition points. The abnormal behaviour of ultrasonic absorption in these polymer solutions may be related to some kind of conformation transition. The increase in the ultrasonic absorption may be ascribed to the abrupt increase in fluctuation in some quantities in the vicinity of such transition point.

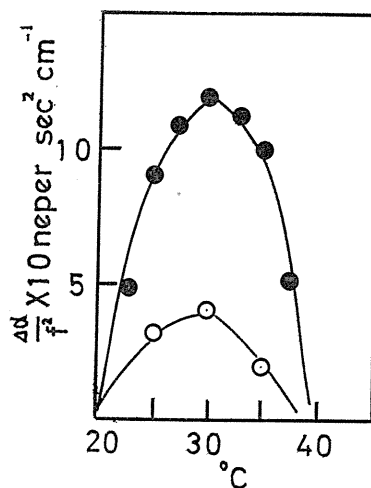


Fig. 45. Temperature dependence of abnormal absorption in P. V. P. - water.
Frequency (MHz) (●); 5MHz, (○); 7MHz

4. 7. Compressional Modulus and Shear Modulus of Polymer Solutions.

In order to compare the ultrasonic data with those of high frequency measurements of shear elasticity, the amount due to the thermal relaxation should be sub-

stracted from the excess absorption coefficients of the solution. The remaining part, $\Delta\alpha'$, is related to $\Delta\kappa' + 4/3\Delta\eta'$ as

$$\Delta\kappa' + \frac{4}{3}\Delta\eta' = \frac{\Delta\alpha'}{f^2} \frac{\rho C^3}{2\pi} = \Delta M'' \quad (48)$$

where it is assumed that $\rho C^2 \approx \rho_0 C_0^2$.

Moore, McSkimin, Gieueishi and Andreath, Jr. (31) have determined the shear modulus, G' and G'' of solutions of polystyrene in dibutylphthalate at 25 °C.

In Fig. 46, the concentration dependence of excess values, $\Delta M''$, $\Delta K''$, and $\frac{4}{3}\Delta G''$

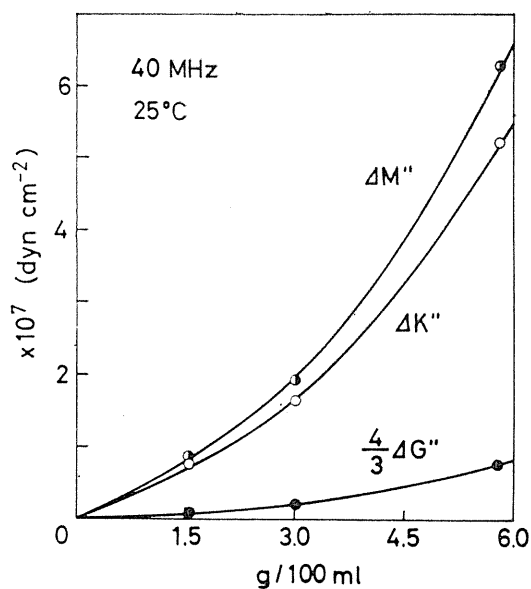


Fig. 46. Concentration dependence of imaginary part of compressional and shear moduli of solutions.
 $\Delta M'' = M'' - M''_0$, $\Delta K'' = K'' - K''_0$
 $\Delta G'' = G'' - G''_0$

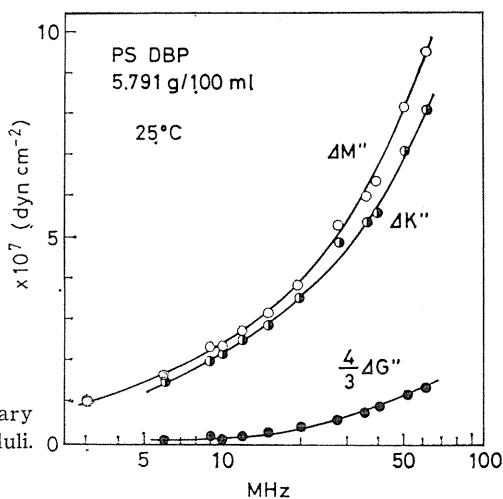


Fig. 47. Frequency dependence of the imaginary part of compressional and shear moduli.
 $\Delta M'' = M'' - M''_0$, $\Delta K'' = K'' - K''_0$
 $\Delta G'' = G'' - G''_0$

at 25 °C and 40 MHz is shown, and in Fig. 47, the frequency dependence of $\Delta M''$, $\Delta K''$, and $\Delta G''$ is illustrated. Since the ultrasonic velocity dispersion is not observed in the polymer solutions, M' is independent of the frequency. The order of magnitude of M' is 10^{10} , while that of G' 10^{6-7} , and the contribution of G' to M' is negligible. As is seen Fig. 46, the compressional modulus and shear modulus increase with increase of concentration. The term of $4/3\Delta G''$ is 10% of that of $\Delta M''$. Therefore, $\Delta M'' \simeq \Delta K'' \gg 4/3\Delta G''$. As is seen Fig. 47, both $\Delta K''$ and $\Delta G''$ increase rapidly above 50 MHz, where the ratio of $\Delta G''$ to $\Delta M''$ increase remarkably.

Ohsawa and Wada (44) have shown empirically that in the frequency range from 10 to 300 KHz, the compressional modulus is overwhelmingly predominant in the longitudinal modulus for the solutions of polystyrene in xylene, and the contribution of shear elasticity to it is negligible.

The temperature dependence of $\Delta\kappa' + 4/3\Delta\eta'$ is shown in Fig. 48. The solid circle in the figure is the values calculated from the experimental results obtained

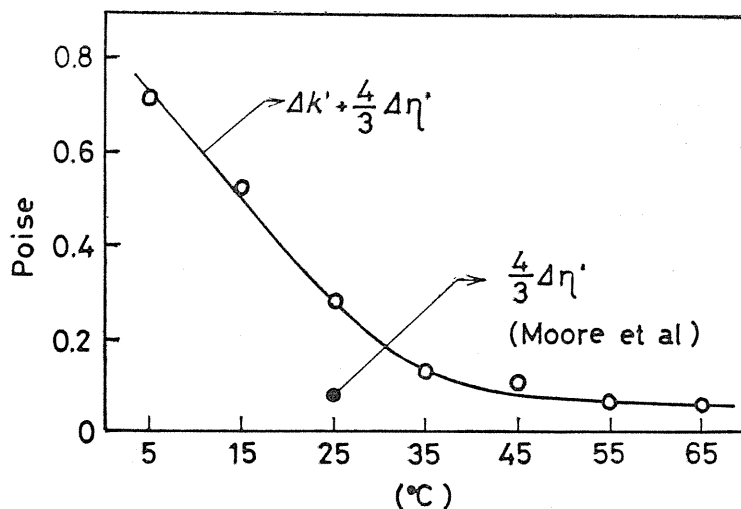


Fig. 48. Temperature dependence of the $\Delta\kappa' + \frac{4}{3}\Delta\eta'$, $\Delta\kappa' = \kappa - \kappa_0'$, and $\Delta\eta' = \eta' - \eta'_0$.

by Moore, McSkimin, Gieueieuski and Andreath, Jr. (31). The ratio $\Delta\kappa'/\Delta\eta'$ is 2.2, and this value is larger than 2/3, which is derived by Okano (47) theoretically.

5. Conclusion.

It is quite lucky that a single relaxation revealed in the ultrasonic absorption in vinyl-type polymer solutions. It is an evidence of existence of some local motions in the back-bone chains of polymer molecules, although their definite model is not yet established.

Our further program to be undertaken concerning this problem is the extension of frequency range to both sides, to higher and to lower, which is still a very

hard project in the experimental technique.

It is hoped by the present authors that the information accumulated centering around on a problem of the ultrasonic absorption in polymer solutions could be much help to the development of polymer science of other branches, such as the science of biopolymers.

References

- 1) Andree, J. H., E. L. Hersell and J. Lamb, *Proc. Phys. Soc.*, B **69**, 625 (1951)
- 2) Bauer, H.-J., H. Hässler, and M. Immendörfer, *Discussions Faraday Soc.*, **49**, 238 (1970)
- 3) Bovey, F. A., F. P. Hood III, E. W. Anderson and L. C. Snyder, *J. Chem. Phys.*, **42**, 3900 (1965)
- 4) Burke, J. J., G. G. Hammes, and T. B. Lewis, *J. Chem. Phys.*, **42**, 3520 (1965)
- 5) Cerf, R., R. Zana and S. Candau, *Comptes Rendus*, **252**, 681 (1961)
Cerf, R., S. Candau and R. Zana, *Zeit. Phys. Chem.*, **65**, 687 (1961)
Candau, S., R. Zana and R. Cerf, *Comptes Rendus*, **252**, 2229 (1961)
Cerf, R., *Comptes Rendus*, **270**, 1075 (1970)
- 6) Cohran, M. A., J. H. Dunber, A. M. North and R. A. Pethrick, *J. Chem. Soc. Faraday Trans. II*, **70**, 215 (1974)
- 7) Davidovich, L. A., A. A. Ivanov, S. Makhkamov, L. Pulatova, P. K. Khabibullaev, M. G. Khaliulin and Sh. Sharipov, *Soviet. Phys.-Acoustics* **19**, 18 (1973)
- 8) Fünfschilling, O., P. Lemaréchal and R. Cerf, *Comptes Rendus*, **270**, 659 (1970)
- 9) Fünfschilling, O., P. Lemaréchal and Cerf, *Chem. Phys. Letters* **12**, 365 (1971)
- 10) Fünfschilling, O., P. Lemaréchal and R. Cerf, *Comptes Rendus*, **270**, 659 (1970)
- 11) Goberman, G., *Nature*, **191**, 693 (1961)
- 12) Hammes, G., G and T. B. Lewis, *J. Phys. Chem.*, **70**, 1610 (1966)
- 13) Hawley, S., A and F. Dunn, *J. Chem. Phys.*, **50**, 3523 (1969)
- 14) Hässler, H., and H.-J. Bauer, *Kolloid-Z.*, **230**, 194 (1969)
- 15) Jujo, Y., M. Saito, H. Ikeda and Y. Masuda, *J. Soc. Rheology, Japan*, **2**, 7 (1974)
- 16) Kato, S., H. Kondo, I. Fujio, H. Nomura, and Y. Miyahara, *J. Chem. Soc. Japan (Chem. & Ind. Chem.)* **1974**, 1981
- 17) Kato, S., H. Nomura and Y. Miyahara to be published.
- 18) Kato, S., I. Uehara, H. Kondo, H. Nomura and Y. Miyahara, *J. Chem. Soc. Japan (Chem. & Ind. Chem.)* **1975**, 1651
- 19) Kato, S., I. Uehara, H. Nomura and Y. Miyahara, *Report Prog. Polymer Phys. Japan*, **18**, 131 (1975)
- 20) Kessler, L. W., W. D. O'Brien, Jr. and F. Dunn, *J. Phys. Chem.*, **74**, 4069 (1970)
- 21) Krigbaum, W. R., F. Mark and J. G. Pritchard, *Makromol. Chem.*, **65**, 101 (1963)
- 22) Lamb, J., "Physical Acoustics" Edited by W. P. Mason, *Acad. Press. Vol. II (Part A)* p 209.
- 23) Lemaréchal, P., *Chem. Phys. Letters*, **16**, 495 (1972)
- 24) Liee, Kang-Jen and R. Ullman, *Polymer*, **6**, 100 (1963)
- 25) Litovitz, A. T., and C. M. Davis, "Physical Acoustics" Edited by W. P. Mason, *Acad. Press. Vol. II (Part A)* p 299.
- 26) Ludlow, W., E. Wyn-Jones and J. Rassing, *Chem. Phys. Letters*, **13**, 477 (1972)
- 27) Masuda, Y., H. Ikeda and K. Kobayashi, *J. Material Soc. Japan*, **19**, 375 (1970)
- 28) Masuda, Y., H. Ikeda and M. Ando, *J. Material Soc. Japan*, **20**, 675 (1971)
- 29) Masuda, Y., H. Ikeda, K. Takeuchi and Y. Jujo, *J. Material Soc. Japan*, **22**, 489 (1973)
- 30) Mikhailov, I., and E. S. Safina, *Soviet Phys.-Acoustics* **17**, 335 (1972)
- 31) Moore, R. S., H. J. McSkimin, C. Gieueuski and P. Andreath Jr, *J. Chem. Phys.*, **47**, 3 (1967), *ibid*, **50**, 5088 (1969)
- 32) Nomura, H., and Y. Miyahara, *Bull. Chem. Soc. Japan*, **39**, 1599 (1966)
- 33) Nomura, H., and Y. Miyahara, *Nippon Kagaku Zasshi*, **88**, 502 (1967)

- 34) Nomura, H., S. Kato and Y. Miyahara, *ibid*, **89**, 149 (1968)
 35) Nomura, H., S. Kato and Y. Miyahara, *ibid*, **90**, 250 (1969)
 36) Nomura, H., S. Kato and Y. Miyahara, *ibid*, **90**, 1218 (1969)
 37) Nomura, H., S. Kato and Y. Miyahara, *ibid*, **91**, 837 (1970)
 38) Nomura, H., S. Kato and Y. Miyahara, *ibid*, **91**, 1042 (1970)
 39) Nomura, H., S. Kato and Y. Miyahara, *J. Material Soc. Japan*, **20**, 669 (1971)
 40) Nomura, H., S. Kato and Y. Miyahara, *ibid*, **21**, 476 (1972)
 41) Nomura, H., S. Kato and Y. Miyahara, *J. Chem. Soc. Japan* (Chem. & Ind. Chem.) **1972**, 1291
 42) Nomura, H., S. Kato and Y. Miyahara, *ibid*, **1973**, 1554
 43) Nomura, H., S. Kato and Y. Miyahara, *ibid*, **1973**, 2398
 44) Ohsawa, T., and Y. Wada, *Polymer J.*, **1**, 465 (1970)
 45) Ono, K., H. Shintani, O. Yano and Y. Wada, *Polymer J.*, **5**, 164 (1973)
 46) Ott, H., R. Cerf, B. Michels and P. Lemaréchal, *Chem. Phys. Letters*, **24**, 323 (1974)
 47) Okano, K., *Reprt. Prog. Polymer Phys. Japan*, **5**, 67 (1962)
 48) Okano, K., *ibid*, **9**, 19 (1966)
 49) Parker, P. C., K. Applegate and L. J. Slutzky, *J. Phys. Chem.*, **70**, 3018 (1966)
 50) Reeves, L. W., and W. G. Schneider, *Can. J. Chem.*, **35**, 251 (1957)
 51) Reiss, C., and H. Benoit, *Comptes Rendus*, **253**, 268 (1961)
 52) Schmidt, A., and A. J. Kovacs, *Comptes Rendus*, **255**, 677 (1962)
 53) Takeda, T., *Bull. Chem. Soc. Japan*, **32**, 1151 (1959)
 54) Teramachi, S., A. Takahashi and I. Kagawa, *Nippon Kogyo Kagaku Zasshi*, **69**, 685 (1966)
 55) Tondre, C., and R. Cerf, *J. Chim. Phys.*, **65**, 1105 (1968)
 56) Wada, Y., and S. Shimbo, *J. Acous. Soc. Amer.*, **25**, 549 (1953)
 57) Wada, Y., G. Tanabe, K. Shiraishi, H. Fujii, T. Sugawara and K. Okano, *17 th Congress of Polymer Science. Tokyo.* (1968) p 465

List of Symbols

A	Chemical species
A	Relaxation parameter
a	Diameter of molecular sphere
B	Relaxation parameter
C	Sound velocity
C	Constant
C_p	Heat capacity at constant pressure
c	Concentration
f	Frequency
f_r	Relaxation frequency
G	Shear modulus
ΔG	Gibbs free energy change of reaction per unit change of ordering parameter
ΔH	Enthalpy change of reaction per unit change of ordering parameter
I	Moment of inertia
\mathcal{I}	Imaginary part
J	Mechanical equivalent of heat, 4.1855 J/cal
K	Compressional modulus
K	Equilibrium constant
k	Rate constant
k	Complex propagation constant
k	Boltzmann constant
L	Length of side chain
M	Longitudinal modulus
m	Number of moles
n	Number of moles

R	Gas constant
\Re	Real part
r	Relaxation strength
r	Distance
S	Entropy
T	Temperature
t	Time
u	Displacement of the material
V	Volume
ΔV	Volume change of reaction per unit change of ordering parameter
Z	Acoustic impedance

(Greeks)

α	Absorption coefficient
β_S	Adiabatic compressibility
β_T	Isothermal compressibility
Γ	Transition probability
γ	Ratio of heat capacity
Δ	Difference symbol
δ	Difference symbol between equilibrium and instantaneous values
ϵ	Parameter of Lennard-Jones potential
η	Shear viscosity
θ	Thermal expansion coefficient
κ	Volume viscosity
λ	Wave length
μ	Absorption per wave length, $\alpha\lambda$
ν	Wave number
ρ	Density
σ	Parameter of Lennard-Jones potential
τ	Relaxation time
ω	Angular frequency, $2\pi f$

(Subscripts)

l	Longitudinal wave
t	Transverse wave
0	Value at equilibrium
0	Solvent
1	State 1
2	State 2
12	From state 1 to 1
21	From state 2 to 2

(Superscripts)

*	Activated state
*	Complex quantity
'	Real part of complex quantity
"	Imaginary part of complex quantity
o	Value at equilibrium
∞	Instantaneous value

Abbreviation

D. M. F.	N-N-dimethyl formamide
M. E. K.	Ethyl methyl ketone

D. B. Ph.	Dibutyl phthalate
D. E. Ph.	Diethyl phthalate
P. C.	Polycarbonate
P. M. A.	Polymethacrylic acid
P. M. M. A.	Polymethyl methacrylate
P. V. Ac.	Polyvinyl acetate
P. V. Bu.	Polyvinyl butylate
P. V. P.	Polyvinyl pyrrolidone
P. V. Pr.	Polyvinyl propionate
P. V. Py.	Polyvinyl pyridone
P. S.	Polystyrene